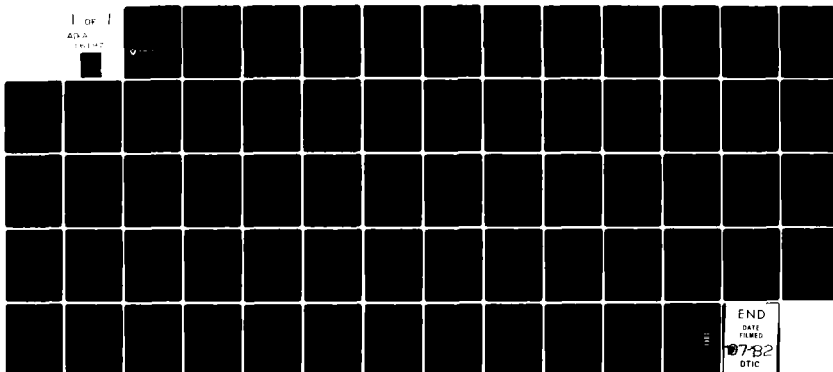AD-A116 197

ARMY ARMAMENT RESEARCH AND DEVELOPMENT COMMAND ABERD--ETC F/G 20/8
COLLISION-INDUCED ENERGY TRANSFER IN THE B STATE OF DIATOMIC SU--ETC(U)
MAY 82   T A CAUGHEY, D R CROSLEY

UNCLASSIFIED   ARBRL-TR-02408   SBI-AD-F300 043   NL
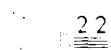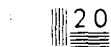
END
DATE
FILMED
07-82
DTIC

AD·F30004
12

AD

TECHNICAL REPORT ARBRL-TR-02408

COLLISION-INDUCED ENERGY TRANSFER IN THE
B STATE OF DIATOMIC SULFUR

Thomas A. Caughey
David R. Crosley

May 1982

US ARMY ARMAMENT RESEARCH AND DEVELOPMENT COMMAND
BALLISTIC RESEARCH LABORATORY
ABERDEEN PROVING GROUND, MARYLAND

Approved for public release; distribution unlimited.

82 06 17 024

REPORT DOCUMENTATION PAGE		READ INSTRUCTIONS BEFORE COMPLETING FORM
1. REPORT NUMBER Technical Report ARBRL-TR-02408	2. GOVT ACCESSION NO. AD-A116 197	3. RECIPIENT'S CATALOG NUMBER
4. TITLE *(and Subtitle)* COLLISION-INDUCED ENERGY TRANSFER IN THE B STATE OF DIATOMIC SULFUR		5. TYPE OF REPORT & PERIOD COVERED
		6. PERFORMING ORG. REPORT NUMBER
7. AUTHOR(s) Thomas A. Caughey* David R. Crosley**		8. CONTRACT OR GRANT NUMBER(s)
9. PERFORMING ORGANIZATION NAME AND ADDRESS US Army Ballistic Research Laboratory ATT: DRDAR-BLI Aberdeen Proving Ground, MD 21005		10. PROGRAM ELEMENT, PROJECT, TASK AREA & WORK UNIT NUMBERS 1L162618AH80
11. CONTROLLING OFFICE NAME AND ADDRESS U.S. Army Armament Research & Development Command US Army Ballistic Research Laboratory (DRDAR-BL) Aberdeen Proving Ground, MD 21005		12. REPORT DATE May 1982
		13. NUMBER OF PAGES 63
14. MONITORING AGENCY NAME & ADDRESS(If different from Controlling Office)		15. SECURITY CLASS. (of this report) Unclassified
		15a. DECLASSIFICATION/DOWNGRADING SCHEDULE

16. DISTRIBUTION STATEMENT *(of this Report)*

Approved for public release; distribution unlimited.

17. DISTRIBUTION STATEMENT *(of the abstract entered in Block 20, if different from Report)*

18. SUPPLEMENTARY NOTES

*Present address: Interactive Radiation, Inc., Northvale, NJ 07647
**Present address: Molecular Physics Laboratory, SRI International, Menlo Park, CA 94025

19. KEY WORDS *(Continue on reverse side if necessary and identify by block number)*

20. ABSTRACT *(Continue on reverse side if necessary and identify by block number)* raj

Rates for collision-induced vibrational and rotational energy transfer within the $3^3\Sigma_u^-$ state of diatomic sulfur are reported. The S_2 was initially excited to $v'=4$, $N'=40$, $J'=41$ by absorption of a Zn atomic line. Fluorescence measurements, made as a function of foreign gas pressure, were used to determine the rates. The collision partners investigated were the five rare gases, H_2, and N_2. In addition, the rate of quenching of S_2(B, $v'=4$) by S_2(X) is reported.

DD FORM 1473 EDITION OF 1 NOV 65 IS OBSOLETE

TABLE OF CONTENTS

3

TABLE OF CONTENTS (Cont'd)

LIST OF ILLUSTRATIONS

5

LIST OF TABLES

7

I. INTRODUCTION

Energy transfer studies of selectively excited diatomic sulfur, investigated by fluorescence techniques, have been known for many years.[1] Using fluorescence progressions excited by mercury line radiation, Rompe[1] observed that changes in the vibrational and rotational levels of the excited state took place prior to emission, if He, Ne or N_2 were mixed with the sulfur vapors. He found little quenching to occur, and noted that $\Delta v = -1$ changes were more likely than $\Delta v = -2$ changes. Heil[2] verified these results using He as a collision partner, and also showed that ground state S_2 was an efficient quencher of the excited state fluorescence. Durand,[3] employing magnesium line excitation, observed changes in vibrational and rotational state due to collisions with rare gases.

While these early studies have clearly established some qualitative features of relaxation processes in $B^3 \Sigma_u^-$ S_2, quantitative rates for a series of gases is lacking. Using photoelectric measurements of intensities of fluorescence, we have determined rates of vibrational and rotational relaxation from a single initially excited state: v'=4, N'=40, J'=41. The collision partners investigated are H_2, N_2, and the five rare gases. Selection of the single excited level is made possible due to the fortuitous overlap of an atomic zinc line at 307.6 nm with a molecular absorption line in the S_2. Although atomic line excitation has the obvious disadvantage, compared to tunable laser excitation, of limiting the generality of the results to only a single initially pumped level, it does offer the advantage of a highly frequency-stable source, allowing intensive measurements of a very reproducible nature to be made. The B-X system is both congested and extensive, requiring long, drift-free scans of low signal intensity for which this lamp stability proved important.

Interest in S_2 lies partly in its suitability as a model molecule, a prototype $^3 \Sigma$ state, for collisional studies; this is largely due to its easy accessibility with selective excitation. Here we report total vibrational transfer rates out of v'=4, the vibrational rates for 4→3 and 4→5, and total rotational transfer rates out of N'=40, J'=41 within v'=4. Measurements have also been made of final-state specific rotational transfer rates from this same initially excited level,[4] and of the degree of retention of orientation of the J-vector following a rotationally

1. R. Rompe, Z. Phys. 65, 404 (1930).

2. O. Heil, Z. Phys. 74, 18 (1932).

3. E. Durand, J. Chem. Phys. 8, 46 (1940).

4. T. A. Caughey and D. R. Crosley, to be published.

inelastic collision.[5] All of these results form component pieces of the picture of the collisional dynamics experienced by B-state S_2.

In addition, the B-X system of S_2 is important from a more applied point of view. It is an ideal candidate for probing combustion systems via laser-excited fluorescence,[6] providing information on the reaction networks for sulfur-containing fuels. Recently, an optically pumped laser operating on the B-X system has been constructed.[7] This offers near-continuous tunability over a wide range using different pump wavelengths; efforts are commencing to obtain laser action using chemical pumping (via inverse predissociation) of S_2.[8] In both of these applications, diagnostics and lasing, data on energy transfer within the B-state is needed not only for a quantitative understanding of the processes involved, but also for less detailed models used to assess and predict proper operating parameters.

II. EXPERIMENTAL DETAILS

The apparatus necessary to carry out this experiment is quite simple in principle. It consists of a light source, a cell containing S_2 which can be filled with the collision partner gases, a monochromator for dispersing emission at right angles to the exciting beam, and a photomultiplier with its associated electronics. As already alluded to, a good deal of care was necessary in the design and operation of these components to ensure reproducible results. In this section are described the lamp, the cell, and the monochromator/detector used for the vibrational and rotational rate measurements. Further details may be found in Ref. 9. Two other cells, used in an investigation of quenching, are briefly described in the section dealing with those measurements.

A. Lamp

An electrodeless zinc atomic emission lamp was constructed from one inch diameter quartz tubing with a quartz window fused onto the end. A cylindrical stainless steel oven within the tube, resistively heated by nichrome wire wrapped around a boron nitride insert, contained Zn granules and controlled the Zn vapor pressure. Ar at $\sim$ 1 torr was flowed continuously over the window and through the lamp, by means of a small vacuum

5. T. A. Caughey and D. R. Crosley, Chem. Phys. 20, 467 (1977).

6. S. R. Leone and K. G. Kosnik, Appl. Phys. Lett. 30, 346 (1977).

7. P. Scott, Xonics, Inc., private communication, 1977.

8. C. H. Muller II, K. Schofield, M. Steinfeld and H. P. Broida, Bull. Amer. Phys. Soc. 23, 74 (1978).

9. T. A. Caughey, Ph.D. Thesis, University of Wisconsin, 1977.

pump. The window was also kept warm by heater wires; these precautions[10] prevented Zn deposits on the window. An A-type antenna coupled power from a 2450 mHz generator into the Zn-Ar mixture. The harmful microwave radiation was shielded by a surrounding mini-box wrapped with aluminum foil covering the lamp; three layers of fine wire mesh screen provided a window through which the Zn 307.6 nm radiation was taken.

The lamp was capable of continuous operation for several days before needing restocking with Zn. Besides the Zn atomic line emission, impurity bands due to CN and ZnH were observed. Though these did not excite the S_2, they occasionally appeared as scatter in the fluorescence spectrum necessitating either corrections or ignoring some wavelength regions in the data analysis.

A small portion of the Zn radiation was split off and its intensity monitored throughout the experiments with a 0.45 m McKee-Pedersen mono-chromator equipped with an RCA 1P28 photomultiplier. The intensity of the lamp would slowly drift during the fifty-minute scans of the vibrational transfer data. The drift ranged from 2 to 10% of the mean intensity; the recorded monitor output was used to correct the data to conditions of constant excitation intensity. Shorter term fluctuations, over the minute or so required to scan over the rotational structure of a single band, were smaller, 1 to 2%.

B. Cell

A T-shaped sulfur cell was made of one inch quartz tubing with the three quartz windows fused into place. A reservoir sidearm containing sulfur was attached to the bottom of the cell; heater coils maintained the temperature (at typically 140°C) to regulate the sulfur vapor pressure. The cell body itself was heated to 630°C, a temperature at which all (> 99%) of the sulfur is in the form of S_2. The collision partner was admitted through a filling port connected to a gas handling manifold, via a graded seal and Kontes high vacuum teflon stopcock. To prevent condensation of sulfur, the stopcock was maintained at 200°C (necessi-tating operation with no seating o-ring on the stopcock). The reservoir temperature is the only one whose control was crucial; its heater windings were powered by a regulated DC supply while Variacs sufficed for the cell body and stopcock coils. Thermocouples provided constant monitors of the temperatures of the three regions.

The cell was filled, at room temperature, with a particular pressure of the collision partner and then heated. With less than a torr of fill gas, the reservoir and body heated up to operating temperature of 140°C and 630°C within a half hour. With higher fill gas pressures in the cell,

---

10. *Efficient coupling was difficult to achieve with this lamp, and it was necessary to force-air cool the connecting cable to prevent it from melting.*

the body continued to heat up to the operating temperature quite rapidly, but the reservoir approached its steady-state temperature sluggishly. The heating period required to attain a constant reservoir temperature increased to a little over one hour with 20 torr and up to three and a half hours with 250 torr pressure.

During the fifty-minute scans, fluctuations could be noted in both the reservoir and body temperatures. The body temperature drifted as much as 5 K and could affect the amount of light absorbed by as much as 1%. The reservoir temperature was constant to within about 0.5 K. This small variation, however, causes about a 5% variation in the sulfur vapor pressure and must be considered a major cause of noise in the data.

The pressure of the fill gas was measured using an NRC Alphatron gauge calibrated for each gas against a cold-trapped MacLeod gauge or mercury manometer. This pressure measurement was made at room temperature, with the fill gas at uniform number density throughout the cell. The experiments are carried out, however, with different regions of the cell at different temperatures. The fill gas pressures are high enough such that the pressure is uniform over the cell, but then the number density is not. We calculate the number density in the cell body by artificially dividing the cell into two distinct regions, one at 200°C and the other at 630°C. While there actually exists a smooth temperature gradient, and three distinct regions corresponding to cell body, reservoir, and stopcock, the fact that the body comprises over 85% of the total cell volume suggests that this approach should be sufficiently accurate.

C. Monochromator/Detector

For the vibrational and rotational relaxation rate measurements, fluorescence was focused onto the slit of a 0.75 m Spex monochromator operated in first order. Spectra were taken using a 100 μ wide entrance slit and a 200 μ wide exit slit. These settings produced an instrumentally determined bandwidth of 0.2 nm, furnishing a reasonable compromise between intensity and resolution of individual vibrational bands. Although individual rotational lines emitted by molecules which have undergone energy transfer collisions are not resolved with these slit settings, the main rotational branches due to the initially excited level are separated by about 0.4 nm (at 300 nm) and are easily resolved.

The detector was an EMI 9558QA photomultiplier tube, cooled to between 0 and 10°C. This cooling slightly increased the sensitivity and, more important, lowered the dark current. It also prevented the hot sulfur cell from increasing the pmt dark current due to convection heating. If the dark current is constant, an accurate baseline can be determined. Since overlapping vibrational bands may obscure the correct baseline for runs in which a moderate amount of vibrational relaxation has occurred, maintenance of a constant temperature photomultiplier is crucial for meaningful intensity measurements.

12

Values for the quantum efficiency as a function of wavelength for the monochromator and detector were obtained from Meyer's relative intensity calibration of this same system.[11] This quantum efficiency determination was carried out using the unpolarized output of a tungsten-halogen secondary emission standard. In the present experiments, using unpolarized exciting light and viewing fluorescence at right angles to the exciting beam, the fluorescence is polarized in an amount of about 3.5%.[12] Using the manufacturer's curves for grating response as a function of polarization shows that the calibration using unpolarized light introduces less than 1% error for the extrema of the range of wavelengths encountered, and is hence adequate.

III. STEADY-STATE EQUATIONS

Fig. 1 exhibits several typical spectral scans recorded to illustrate the evolution of the emission spectrum as the pressure of the collision partner - in this case, argon - is increased. At zero Ar pressure, the spectrum consists entirely of those fluorescent lines emitted by the initially pumped level; the (4,5) through (4,12) terms, with their characteristic Franck-Condon pattern, can be seen in this region. Each term is observed as three lines. The two stronger ones are the R_1 branch and the blended P_1 and $^PR_{13}$ branches, while the weak line is the $^NP_{13}$ branch.[13] The scan at 5.5 torr exhibits substantial filling in of the (4,v'') bands, due to rotational transfer, and the presence of other (v', v'') bands emitted by molecules which have undergone vibrational transfer collisions. However, a substantial number of molecules still remain in the initially excited level, as can be seen from the characteristic pattern in the (4,v'') bands. As the Ar pressure is increased, further relaxation occurs until at 170 torr most of the molecules are in v'=0 or 1. Even at this pressure, however, there remains noticeable emission from the initially excited level, most evident for (4,6) and (4,10).

From measurements of these intensities, one may obtain relative populations of individual vibrational levels, and of transferred rotational levels in v'=4 ($\Delta v'=0$, $\Delta N' \neq 0$) as compared to the population of the initially excited level. This procedure is described below in the pertinent sections. These populations, as a function of pressure, may then be used to extract rate constants for the energy transfer processes.

We here present short derivations of the equations used for the rate constant analysis. Definitions of the notation utilized are collected

11. K. A. Meyer, Ph.D. Thesis, University of Wisconsin, 1976.

12. K. A. Meyer and D. R. Crosley, J. Chem. Phys. 59, 1933 (1973).

13. K. A. Meyer and D. R. Crosley, Can. J. Phys. 51, 2119 (1973). The spectroscopic notation is as follows, with $\Delta J = J'-J''$ and $\Delta N = N'-N''$: R_1, $\Delta J=\Delta N=1$; P_1, $\Delta J=\Delta N=-1$; $^PR_{13}$, $\Delta J=-1$; $\Delta N=1$; $^NP_{13}$, $\Delta J=-1$, $\Delta N=-3$.
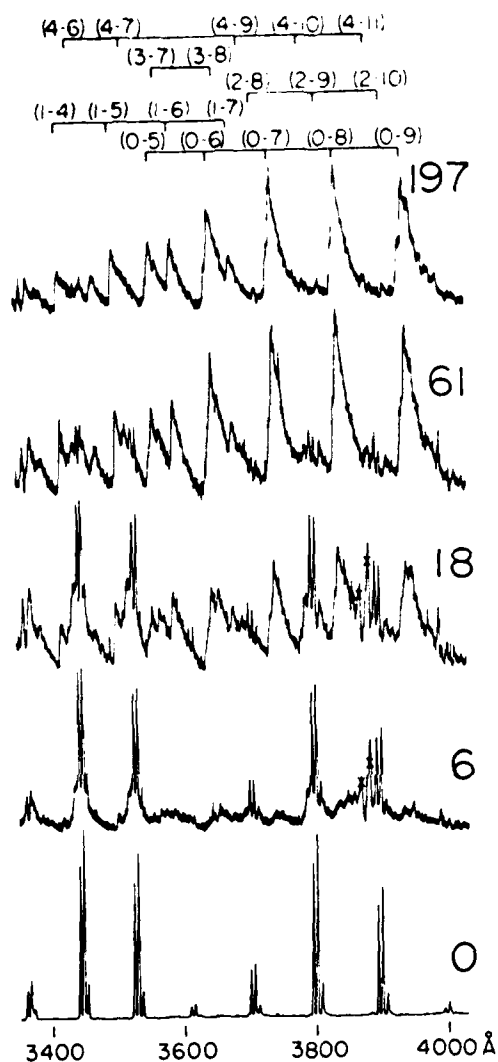
Figure 1. Scans at several pressures of argon showing the evolution of the fluorescence spectrum of S_2 due to rotational and vibrational transfer. The large number by each scan is the pressure of argon in torr, measured at the time of filling the cell (see text; the actual pressure in the hot cell is about three times as much). Several of the bands in this spectral region are marked at the top. The characteristic three lines in each band, seen in the zero-pressure scan, are faintly evident even at the highest pressures. The lines marked with an X are impurity lines from the lamp.

14

In Table 1. All of the equations are obtained by a straightforward steady-state approximation applied to the population of each excited level. This treatment closely parallels that developed by Steinfeld[14] for the analysis of energy transfer in selectively excited I_2.

In the absence of any foreign gas, the balance of absorption with radiation and quenching yields

$$k_a S = \frac{1}{\tau} S^* + Q_s SS^*. \tag{1}$$

Defining the fluorescence intensity as the number of emissions per cm^3 per sec, or $I_0 = S^*/\tau$, we may rearrange to obtain the working equation

$$I_0 = k_a S / (1 + Q_s' S). \tag{2}$$

This will be used to obtain the sulfur self-quenching rate, which enters into all of the rate equations. While we do not actually measure an absolute value for I_0, only relative values are needed to determine Q_s'.

Were they to be significant, terms similar to Q_s' would need to be included to account for vibrational and rotational transfer within B-state S_2 due to collisions with X-state S_2. However (see below), quenching is the only experimentally observable result of an $S_2^* - S_2$ collision; so we shall ignore such self-transfer in the ensuing set of equations.

In the presence of some added gas, another term added to Eq. (1) describes the total excited state density:

$$k_a S = \frac{1}{\tau} S^* + Q_s SS^* + QAS^*. \tag{3}$$

This is rewritten as

$$k_a S / I_A = 1 + Q_s' S + Q'A$$

and combined with Eq. (2) to obtain the working equation used to extract Q':

$$I_0 / I_A = 1 + [Q'/(1 + Q_s' S)]A. \tag{4}$$

14. J. I. Steinfeld and W. Klemperer, J. Chem. Phys. 42, 3475 (1965).

TABLE 1. NOTATION FOR STEADY-STATE EQUATIONS

NOTATION	QUANTITY	COMMENTS/ASSUMPTIONS	UNITS
S	density of ground state S_2		cm^{-3}
A	density of added gas		cm^{-3}
S^*	total excited state density		cm^{-3}
S_v^*	population of $v'=4$ level		cm^{-3}
S_R^*	population of $v'=4$, $F_1(40)$		cm^{-3}
$S_{v_f}^*$	population of transferred S_2	$v_f = 3$ or 5	cm^{-3}
Q_s	self-quenching rate constant	independent of v'	$cm^3\ sec^{-1}$
Q_s'	self-quenching rate constant	$Q_s' = Q_s \tau$	cm^3
V	transfer rate, $v'=4$ to all v_f		$cm^3\ sec^{-1}$
V'	transfer rate, $v'=4$ to all v_f	$V' = V\tau$	cm^3
V_{v_i,v_f}	transfer rate, $v_i=4$ to v_f	$v_f = 3$ or 5	$cm^3\ sec^{-1}$
v'_{v_k,v_f}	transfer rate, $v_i=4$ to v_f	$V'_{v_i,v_f} = V_{v_i v_f} \tau$ J'_f within $v'=4$	cm^3
R	transfer rate, $J'=41$ to all J'_f		$cm^3\ sec^{-1}$
R'	transfer rate, $J'=41$ to all J'_f	$R' = R\tau$	cm^3
Q	quench rate for added gas	independent of v'	$cm^3\ sec^{-1}$
Q'	quench rate for added gas	$Q' = Q\tau$	cm^3
τ	radiative lifetime	independent of level	sec^{-1}
k_a	absorption rate per ground state S_2	contains excitation intensity	sec^{-1}
I_o	fluorescence intensity at zero density	$I_o = S^*/\tau$ for $A=0$	$cm^{-3}\ sec^{-1}$
I_p	fluorescence intensity with added gas	$I_p = S^*/\tau$	$cm^{-3}\ sec^{-1}$

16

In order to investigate total vibrational transfer from the initially excited (v'=4) level, the steady state approximation is applied to that level:

$$k_a S = \frac{1}{\tau} S_v^* + Q_s SS_v^* + QAS_v^* + VAS_v^* . \tag{5}$$

This may be combined with Eq. (3), after multiplying each through by τ, to yield

$$(1 + Q_s'S + Q'A)(S^* - S_v^*) = V'AS_v^*$$

or, in the form used to determine V',

$$(1 + Q_s'S + Q'A)(S^*/S_v^* - 1) = V'A \tag{6}$$

since both Q_s' and Q' have been measured.

In practice, for the pressure regimes over which the experiments are carried out, we must consider the effects of "back-transfer," that is, secondary collisions which transfer the S* back into the initially excited v'=4 level from other levels populated by the first collision. This requires consideration of vibrational transfer rates specific to final vibrational levels. We apply the steady-state balance to vibrational level v_f. It is not pumped by the light source, but is assumed populated only by collisions from v'=4.

$$V'_{v_i,v_f} AS_v^* = (1 + Q_s'S + Q'A + V'A)S^*_{v_f} .$$

We have set the total vibrational relaxation rate of level v_f equal to V' and imposed the same constraint on Q_s, Q and τ. Then

$$(1 + Q_s'S + Q'A + V'A)(S^*_{v_f}/S_v^*) = V'_{v_i,v_f} A . \tag{7}$$

We may now use these values to obtain a back transfer correction to Eq. (6). It is found experimentally (see below) that transfer to adjacent levels ($v_f = 3$ and 5) constitutes a large fraction of the total vibrational transfer (between 62 and 83%, depending on the collision partner). We thus consider only back-transfer from these levels, and include it explicitly. This adds to the left hand side (the input side) of Eq. (5) the terms

17

$$V_{3,4}S_3{}^*A + V_{5,4}S_5{}^*A .$$

We rearrange and combine to obtain the version of Eq. (6) with back-transfer

$$(1 + Q_s'S + Q'A)(S^*/S_v{}^* - 1) + (V'_{3,4}S_3{}^*/S_v{}^* + V'_{5,4}S_5{}^*/S_v{}^*) = V'A \qquad (8)$$

(recalling that $S_v{}^*$ is equivalent to $S_4{}^*$). $V_{3,4}$ and $V_{5,4}$ are approximated by $V_{4,5}$ and $V_{4,3}$, respectively; the results are cycled through Eqs. (7) and (8) until consistent values are obtained.

In a completely analogous way, the total rate of rotational relaxation, within $v'=4$, of the initially excited $N'=40$, $J'=41$ level is obtained.

$$k_aS = \frac{1}{\tau} S_J{}^* + Q_sSS_J{}^* + QAS_J{}^* + VAS_J{}^* + RAS_J{}^* .$$

This is combined with Eq. (5) and rearranged.

$$(1 + Q_s'S + Q'A + V'A)(S_v{}^*/S_J{}^* - 1) = R'A .$$

This equation does not need modification for <u>rotational</u> back transfer, since only a small fraction of the molecules transferred out return to the initially pumped level. However, <u>vibrational</u> back transfer must be taken into account. While the vibrational transfer <u>out</u> of $v'=4$ affects all rotational levels equally, vibrational back transfer <u>in</u> will most likely populate a rotational level other than the one initially pumped. Hence, it should be included in the steady state expressions as an input term to $S_v{}^*$, but forms a negligible portion of the total input for the population $S_J{}^*$. Making this correction then yields the actual working equation

$$(1 + Q_s'S + Q'A + V'A)(S_v{}^*/S_J{}^* - 1)$$

$$- (V'_{3,4}S_3{}^*/S_J{}^* + V'_{5,4}S_5{}^*/S_J{}^*)A = R'A . \qquad (9)$$

The negative sign in front of the back-transfer term (in contrast to the positive sign in Eq. (8)) is due to this consideration of it as an input to $S_v{}^*$ but not $S_J{}^*$.

18

All of the above equations are written such that the experimentally determined quantities are measured on a per radiative lifetime basis. This emphasizes the fact that it is this unit which defines the observational time scale, so that events occurring on the order of tens of nanoseconds are readily probed. In order to obtain absolute rates, however, a value for this radiative lifetime is necessary. We use the value obtained from recent Hanle effect measurements on the same initially pumped state, $v'=4$, $N'=40$, $J'=41$, of 36 nsec.[15] While it is clear that the lifetime is similar[15] for a similar value of J' in $v'=5$, it appears[15,11] to be different for a smaller value of rotation ($J'=13$) within $v'=4$. It is not known whether this is a general trend, or if there is some perturbation in the lower lying rotational level. Our analysis equations presume the same value of lifetime (as well as rates) for all levels involved. A time-domain experiment,[16] which averages over many levels, has obtained a value of 45 nsec; so we consider the value of 36 nsec more representative of the levels probed in our experiments. This value is then adopted as the single τ used in the analysis.

Our approximations, namely the independence of transfer rates and radiative lifetimes for different levels, remove the strict validity of our equations. They should not, however, significantly impair the analysis since we do not anticipate strong dependencies of any of the quantities. The state dependence of such processes, of course, is an active and interesting area of current research.

IV. QUENCHING AND RELATED EXPERIMENTS

A. Self-Quenching

The self-quench rate Q_s enters into all of our steady state equations. Therefore, in addition to the intrinsic interest in this quantity itself, it is necessary to first determine the value of Q_s in order to use it in subsequent analysis procedures.

If the S_2 pressure is low enough, Eq. (2) with a constant value of the absorption coefficient k_a describes the intensity of fluorescence as a function of S. However, a value of Q_s' can be determined only if I_0 deviates noticeably from a strictly linear dependence on S. In practice, this requires operation at high enough values of S such that significant attenuation of the exciting radiation occurs as it passes through the fluorescence cell. This may be readily handled if

---

15.   T. A. Caughey, K. A. Meyer and D. R. Crosley, to be published.

16.   T. H. McGee and R. E. Weston Jr., Chem. Phys. Lett. 47, 352 (1977).

we adopt an empirical view of k_a as a function of S; we separately measure $k_a(S)$ and then measure the intensity of fluorescence per absorbed photon. The working version of Eq. (2) becomes, with c some constant,

$$I_o/k_a(S) = cS/(1 + Q_s'S). \qquad (10)$$

$k_a(S)$ was determined from measurements of the attenuation of the Zn line through a cylindrical cell of 7.5 cm length. The radiation passing through the cell at 307.6 nm was measured by a Heath 0.35 m monochromator, yielding an instrumentally determined linewidth, and the 0.45 m monochromator was used as a lamp monitor. Readings taken with the cell body hot and the reservoir cold were used as 100% transmittance values, and readings with the lamp blocked as 0%.[17] The fluorescence as a function of S was measured using a sealed-off T-shaped cell and a filtered[18] RCA 1P28 photomultiplier detecting the light emitted at right angles to the exciting beam; again the lamp was monitored.

Sulfur vapor pressures above the liquid in the reservoir were calculated from data compiled in Ref. 19. Because the reservoir and the cell body are at two different temperatures, it is necessary to take into account the flow conditions (hydrodynamic or molecular) between the two regions in order to correctly determine the sulfur pressure in the cell body. As is seen below, the hydrodynamic limit forms a safe approximation for our cell and sulfur pressures above about 0.1 torr. The pressure of S_2 within the cell is calculated for this high pressure idealization. Further details and a discussion of flow limits are given in Ref. 9.

Our measured function $k_a(S)$ now may be inserted into Eq. (10), except for some residual concern about the proper determination of the sulfur pressure (in particular, the choice of flow conditions). The experimental results are examined in the following way. First, an absorption coefficient k_o appropriate for continuum radiation is calculated using a lifetime of 36 nsec,[15] the measured Franck-Condon factor for the (4,1) band,[20] the rotational line strength[13] and the appropriate partition

17. *This procedure allows for a dark current correction and avoids changes in the quartz window transmission with temperature.*

18. *10 cm of 0.23N CuSO4 plus a glass filter similar to Corning 7-60, yielding a passband between 320 and 400 nm.*

19. *A. N. Nesmainov, Vapor Pressure of the Chemical Elements, (Elsevier, New York), 1963.*

20. *K. A. Meyer and D. R. Crosley, J. Chem. Phys 59, 3153 (1973).*

functions. The calculated result $k_Q = 0.33$ cm^{-1} torr^{-1} is then compared to the observed value by a computation of the expected absorption from a line source, according to the prescription for exactly overlapping lines given in Mitchell and Zemansky.[21] The comparison indicates[9] a line center mismatch of about 0.03 cm^{-1}. This is a reasonable result for the line overlap, and supports the validity of the method used to determine $k_a(S)$, and the sulfur pressure.

In particular, our approximation of hydrodynamic flow is valid. Were we actually in the molecular flow limit, the k_Q as determined from the experiment would have been higher by a factor of 3.1 owing to the different actual S_2 density. This would be unrealistic when compared with the calculated value in the manner described. On the other hand, the apparent $k_a(S)$ becomes larger below a sulfur pressure of about 0.10 torr,[9] which is where the flow is expected to make a transition from hydrodynamic to molecular conditions. That regime is unimportant in the determination of Q_s', and we conclude that our choice of flow conditions leads to no uncertainty in Q_s'.

For the analysis of the fluorescence data according to Eq. (10), we consider, using our $k_a(S)$, the amount of absorption occurring only in that region of the cell viewed by the photomultiplier, since there is noticeable attenuation through the cell. Additionally, a small correction (1.4% at the highest pressure used) must be applied to account for the fluorescence within the filter passband[18] which is reabsorbed by the S_2 between the emitting region and the viewing window.

The data, expressed in the form of Eq. (10), is graphed in Fig. 2. A non-linear least squares fit yields a value of Q_s' for this experiment.

The sealed-off quartz cell used to obtain these fluorescence data was later shown, using Hanle effect measurements,[15] to contain a foreign gas. The effective lifetime in that cell is shorter, by 23%, due to collisional broadening by the contaminant, compared to collision-free B-state S_2. Applying this correction to obtain Q_s' on a per radiative lifetime basis, we obtain as the final result 1.5 ± 0.3 torr^{-1} τ^{-1}. Alternatively expressed, this is a rate $Q_s = (13 \pm 3) \times 10^{-10}$ cm^3 sec^{-1}, or a cross-section σ_Q of 180 ± 40 Å^2.

Hanle effect broadening rates, separately measured, for S_2S_2 collisions,[4] yielded a coherence destruction cross section σ_{cd} of $210 \pm$ Å^2 for this level. We have ascribed this to quenching collisions

21. A. C. G. Mitchell and M. W. Zemansky, *Resonance Radiation and Excited Atoms*, (Cambridge Univ. Press, Cambridge) 1961.
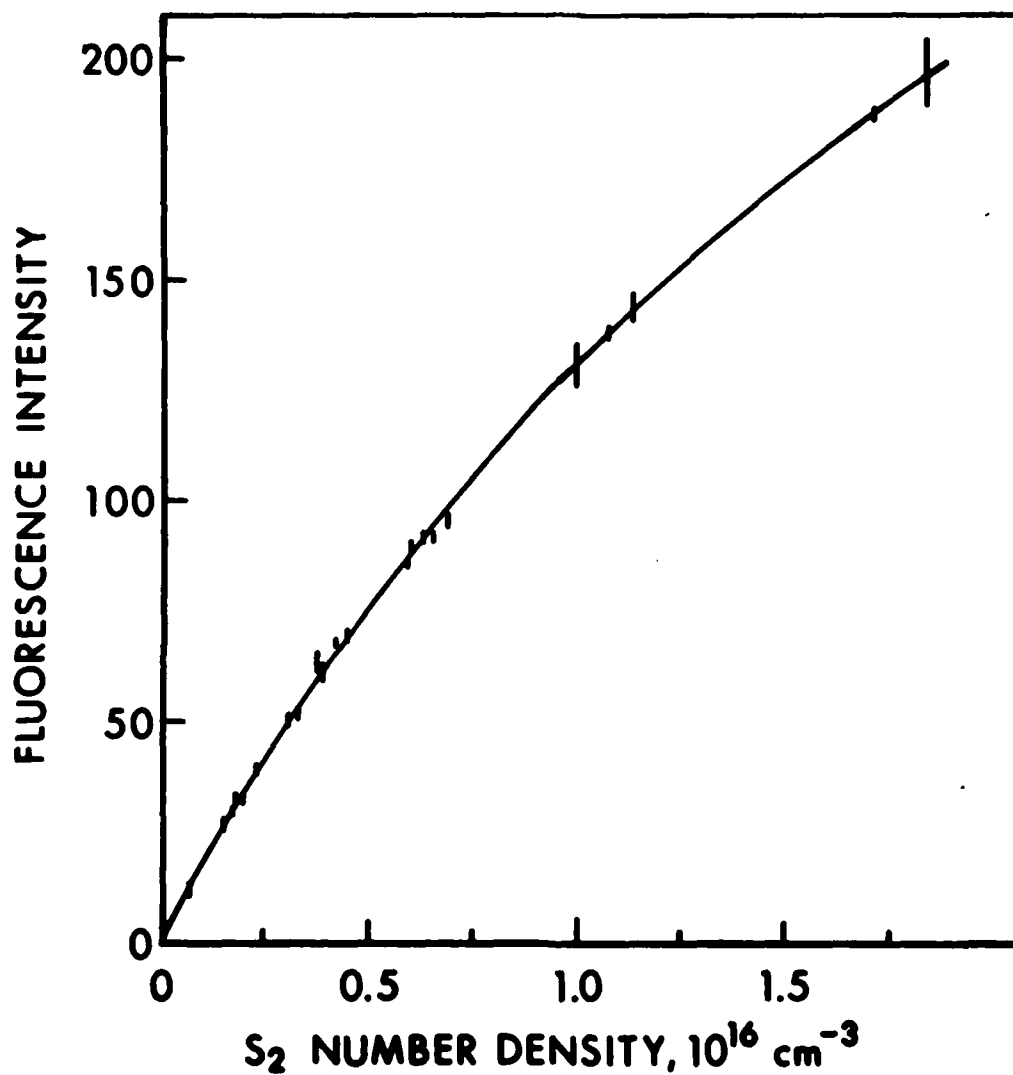
Figure 2. A plot of the fluorescence intensity in arbitrary units vs. number density of S_2. Error bars are indicated, and the curve is a non-linear least squares fit to Eq. (10).

22

only,[22] given the lack of self-transfer (see below); thus these results can be directly compared with one another. We feel they exhibit good agreement for these two distinctly different methods of measuring the same quantity. McGee and Weston,[16] on the other hand, have used broadband excitation and single photon time correlation to obtain a $\sigma_Q = 81 \pm 5$ $\overset{\circ}{A}{}^2$ from the effects of S_2 pressure on the total fluorescence. We can find no obvious reasons for the discrepancy. In what follows, we adopt our own value of Q_s' for insertion into the energy transfer analysis equations.

B. Self-Energy Transfer

A complete accounting for $S_2(B)$ - $S_2(X)$ collisions also requires terms for self-transfer to be considered in Eq. (4) - (9). These processes were studied using fluorescence dispersed by the 0.75 m monochromator. Now, because the quenching rate is large, little fluorescence from transferred molecules would be expected in any case. At relatively high pressures (> 0.7 torr) of S_2, secondary (minor) fluorescence series excited by other Zn lines also appear in the spectrum, further complicating the search for self-transfer. The results are analyzed in the same way as described below for the experiments with other collision partners, except that only three pressures of S_2 were used.

No evidence of vibrational transfer due to S_2-S_2 collisions could be discerned. Considerations of the noise present permit an upper limit estimate of 0.25 Q_s' to be placed on the rate for this process. Some slight filling-in of the $v'=4$ terms could be observed at the highest S_2 pressures. The data[9] yield an estimate of the self-rotational transfer rate as $(4 \pm 3) \times 10^{-10}$ cm^3 sec^{-1}. Some of the emission intensity attributed to rotationally transferred molecules is likely due to the secondary series; hence the true value probably lies nearer the lower error bar limit.

Since the degree of self-transfer is small,[21] we will not include it in what follows. The resulting uncertainties are also small, since we carry out the remaining experiments at as low an S_2 pressure as possible (typically 0.15 torr) in order to minimize such effects. At this pressure, the uncertainty in Q_s' leads to an uncertainty of 0.4% in the final absolute rates, and even less in the relative rates from gas to gas. Our assessment of the effects of the neglect of self-transfer suggests about a 1% uncertainty in the final absolute rates, and even less in relative vibrational and rotational rates.

---

22. It could be argued that the presence of non-zero self-transfer, together with a lack of coherence retention for S_2-S_2 collisions, is what causes the σ_{cd} of Ref. 4 to be slightly greater than the σ_Q measured here. While the difference between them is about the right size, the two values overlap to within their error bars and such an interpretation is tenuous.

23
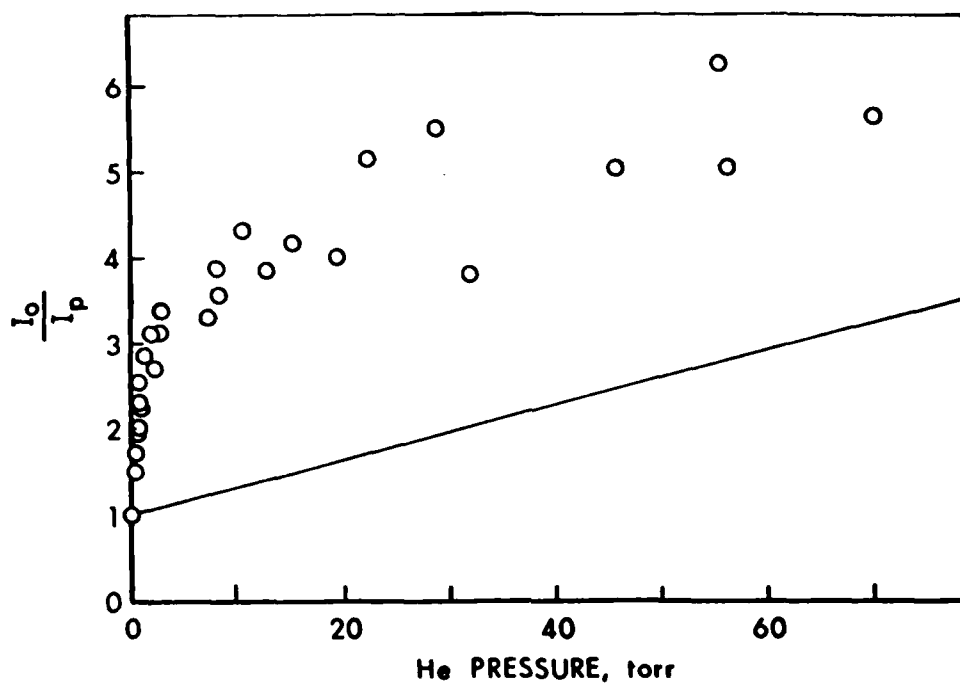
Figure 3. The inverse of the fluorescence intensity, in arbitrary units, versus He pressure, showing the sharp drop in fluorescence at lower pressure and more gradual fall-off at higher pressure. The straight line corresponds to the prediction of a Stern-Volmer curve neglecting the initial sharp fall-off (see text).

24

C. Effects of Rare Gases on Total Fluorescence

It was originally anticipated that a conventional Stern-Volmer plot, in the form of Eq. (4), could be used directly to obtain Q' for the added gases. It quickly became apparent, however, that the dependence of the fluorescence intensity as a function of pressure was quite different from the predictions of this equation.

The essential data is illustrated in Fig. 3 for the case of helium as a fill gas; plotted is the ratio of the intensity at zero-pressure to that at some given pressure. As He is added to the cell, the intensity drops precipitously between zero and about 5 torr, and then falls off more gradually with further increase in pressure. Very similar behavior was also directly measured for Ar as a fill gas. In addition, from similarities in the vibrational transfer data, we infer that the other rare gases, N_2 and H_2 all cause such behavior of the total fluorescence intensity, although the magnitude of the sharp rise decreases with increasing mass of the collision partner.

We consider first the initial sharp rise in I_o/I_p. This cannot be due to collisional quenching of the B state since then the vibrational energy transfer plots, described below, would show a significant departure from linearity. Absorption measurements using the refillable cell quickly revealed that the sharp fall in I_p was due to a sharp (and quantitatively identical) decrease in the amount of Zn line radiation absorbed by the S_2, upon addition of the fill gas. For example, at $S_2 \sim 0.15$ torr, 14% of the 307.6 nm radiation is absorbed at $P(He) = 0$, but at $P(He) = 5$ torr no absorption was detectable above the 3% noise level.

In order to investigate this phenomenon, an extensive series of experiments was carried out using both the refillable cell described in the Experimental Details section, and another cell with a stopcock between the cell body and the sulfur reservoir. This latter cell permitted the body to be maintained with a particular S_2 number density, at a nearly uniform temperature and isolated from the reservoir of liquid sulfur.

The measurements and observations, most of which were carried out with He as the added gas, are described in detail in Ref. 9. Our conclusions from these experiments are several. Neither pressure broadening nor shifting of the molecular absorption line is sufficiently large to account for the decrease in I_p seen in Fig. 3. In the experiments involving the single-stopcock cell, the gaseous and condensed sulfur were always in contact. There, I_p decreased upon addition of He but increased to its original value when the He was pumped out, with the sulfur reservoir always held at the same temperature. The two-stopcock cell was used in particular in the following way. With the valve between cell body and reservoir open, I_p showed the usual decrease upon the addition of He. The stopcock was then closed, isolating the cell body (containing both gaseous sulfur and He) from the reservoir. Upon pumping out the He,

25

I_p remained constant. This demonstrates that the added gas decreases the total number density of gaseous sulfur in the cell above the reservoir containing condensed sulfur, but does not affect the molecular composition of the sulfur vapor.

For the cases of Ar and the heavier gases, a change in flow conditions (molecular to hydrodynamic) can account for the bulk of the change observed. For He, at least, this effect is not sufficient and another phenomenon is contributing. We speculate that the added gas might affect the phase composition within the reservoir, thus changing the total sulfur vapor pressure above the condensed phase at a given temperature. However we have no data bearing directly on this point.

We recall that it was earlier established that the change in I_p was caused directly by a change in the amount of absorption. Thus these experiments have demonstrated that the number density of gaseous sulfur, above a reservoir containing condensed sulfur, is decreased upon the addition of a foreign gas. We emphasize that the observations have not provided an unambiguous explanation for this phenomenon. Most important for the current purpose, however, is that these experiments combined with observations on the vibrational energy transfer data show that the only effect is the lowering of the sulfur number density. Identical after its removal; and the total intensity at a given pressure is simply scaled as the curve in Fig. 3, in the presence of He. Thus we conclude that this phenomenon has no effect on the energy transfer results, when analyzed in terms of population ratios by means of the equations listed above.

The more gentle rise in the I_o/I_p plot of Fig. 3, and the corresponding rise for the Ar experiments, could be due to quenching of the B-state S_2 by the rare gases. They are of a size well consistent with an upper bound estimate to Q' based on vibrational relaxation data described below. In fact, Q' values obtained directly from this slow rise, treated in a Stern-Volmer manner, are $\sim$ 0.2 of those upper bounds. Due to possible problems in so interpreting only the high pressure portion of Fig. 3, in view of our lack of understanding of the low pressure part, we prefer the much larger upper bounds with this suggestion that the true Q' may well be much smaller.

V. VIBRATIONAL TRANSFER

In this section, transfer spectra such as those shown in Fig. 1 are analyzed to determine steady-state vibrational populations as a function of fill gas pressure. This information is then used to calculate vibrational transfer rates using Eqs. (7) and (8), and to follow the overall evolution of the population distribution with increasing fill gas pressure. The data are used to set upper bounds on quench rates, and rotational contours of transferred vibrational bands are examined for information about rotational memory following a collision which alters the vibrational state.

A. Population Determinations

Fig. 4 shows a portion of the fluorescence spectrum emitted in the presence of 18 torr Ar. The band heads are identified by the tabulated positions given by Pearse and Gaydon,[23] which are based mainly on the classic work of Fowler and Vaidya.[24]

The area under each identifiable vibrational band was determined graphically. Because of overlapping, as is evident in Fig. 4, it was necessary to extrapolate the tails of some bands past the heads of those adjacent bands at longer wavelength. In other cases, it was necessary to consider only total contributions from more than one band. The consistency of the band shapes, the inclusion of different overlapping combinations, and the overall redundancy of the data compared with the number of fitted populations (see below) give us confidence that this is a reliable procedure for determining vibrational populations. In this connection, Fig. 4 illustrates the requirement of maintaining a constant, definable baseline throughout a run.

For an isolatable band (v',v''), its area $a_{v'v''}$ is related to the population of the v' level, $n_{v'}$, through the equation

$$n_{v'} \, q_{v'v''} \nu^3 \, \epsilon/\tau = a_{v'v''} \, . \tag{11}$$

Here, $q_{v'v''}$ is the Franck-Condon factor for the band in question, ν is the transition frequency, and ϵ is the detector quantum efficiency at ν, on a current per photon basis. As before, the radiative lifetime τ is assumed independent of v'. For the situation in which more than one band contributes to a given area, the area is a sum of the appropriate terms[25] on the left-hand side of Eq. (11). Values of $q_{v'v''}$ are taken from the measurements of Meyer[11,20] for $v'=3,4$ and 5; calculations by Brabson[26] using RKR potentials furnished $q_{v'v''}$ for $v'=0,1$ and 2. These parameters, and the product[25] $f^v_{v',v''} = q_{v'v''} \epsilon \nu^3$ for each band

23. R. W. B. Pearse and A. G. Gaydon, *The Identification of Molecular Spectra*, 3rd Ed. (Chapman and Hall, London, 1965).

24. A. Fowler and W. M. Vaidya, Proc. Roy. Soc. *A 132*, 310 (1931).

25. *The notation following implicity labels each area by the (v',v'') band forming the dominant contribution.*

26. G. D. Brabson and R. L. Volkmar, J. Chem. Phys *58*, 3209 (1973); G. D. Brabson, private communication (1973).
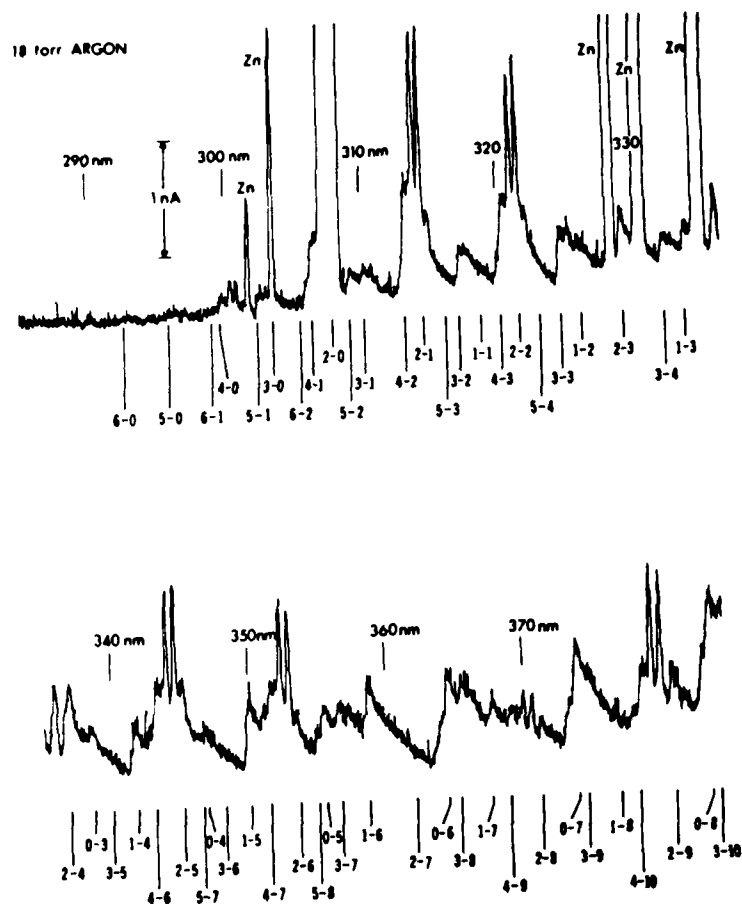
Figure 4. An experimental scan at 18 torr Ar pressure; from scans such as these the vibrational populations are extracted. Positions of the heads of the bands used for analysis are marked. The very high intensity in the region of the (4,1) band is scatter from the exciting Zn line.

28

measured, are collected in Ref. 9. In all, in the wavelength region monitored by the spectrometer, we measure areas corresponding to contributions from between 9 and 12 bands for each v' in the range $0 \leq v' \leq 5$.

At least squares determination of the populations is suggested by the redundancy of the data together with the fact that several areas represent contributions from more than one band. In matrix notation,

$$\underset{\sim}{F}\vec{N} = \vec{A} \, ,$$

where $\vec{N}$ is the column vector of the populations $n_{v'}$, $\vec{A}$ is the column vector of the areas $a_{v'v''}$, and $\underset{\sim}{F}$ is the matrix of the $f^{v'}_{v',v''}$. The unweighted least squares solution is

$$\vec{N} = (\underset{\sim}{F}^{t}\underset{\sim}{F})^{-1}F^{t}\vec{A} \, ,$$

where t denotes transpose and -1 signifies inversion.

Depending on the spectral scan and degree of vibrational overlap, the problem consisted of from 14 to 22 equations in the six unknown $n_{v'}$. As a gauge of the goodness of the fits, the least squares solutions were used to calculate the band areas and usually reproduced the measured values to within 10%.

Several comments concerning possible systematic errors in this method can be made. The largest uncertainty, insofar as transfer rate determinations are concerned, must be in S_2 pressure fluctuations and the Franck-Condon factors since the transition frequencies, detector efficiency, and errors in the measurement of the areas lead to a combined uncertainty of only two or three per cent. Although the RKR Franck-Condon factors for v'=0 and v'=1 agree fairly well with the experimental values of Meyer,[11] especially for the more intense bands, the calculated $q_{v'v''}$ do deviate significantly from those of many of the weaker bands measured by Meyer. However, since primarily the strongest bands will determine the population calculated for the state, the uncertainty in the $q_{v'v''}$ for the weaker bands are of less significance. Since we have no measured values for $q_{2,v''}$, it is more difficult to assess the accuracy of these RKR-calculated terms. However, we expect the vibrational overlap integral to be more sensitive to the more rapidly varying vibrational wavefunction of the v'=2 state than that of the v'=0 or v'=1 state. Indeed, we find that the least squares fits yield a population of v'=2 often larger than can reasonably be expected. Also, the lack of a smooth trend in the population of v'=2 with increasing mean pressure (in contrast to the smooth variations found for the rest of the vibrational levels) makes

29

us believe that n_2 is not as well determined as the others. The cause of this instability is that nowhere in the spectrum is a strong vibrational band of $v'=2$ free from extensive overlapping with other bands or lamp emissions. Hence, the anomalous size of n_2 found in some of the fits[9] should be considered spurious.

We have earlier remarked about the assumption that τ is independent of v'. Another quantum level dependence of concern here is that of the $q_{v'v''}$ on J'. Meyer[11] has found for $v'=5$ that differences of as much as 50% exist for the strongest vibrational bands, when comparing $J'=13$ and 69. However, much less dependence on J' should be noticeable[11] for $J' \leq 50$, which is the range of rotational quantum number significantly populated here.

Although a small amount of fluorescence was sometimes observed emanating from $v'=6$ and $v'=7$, we could not calculate the population of these levels since we lacked reliable Franck-Condon factors. Based on a measurement of the $V'_{4,5}$ rate constant (see below), the assumption that $V'_{5,6} \sim V'_{4,5}$, and the fitted n_5, we expect the largest value of n_6 to be only a few per cent of the total B-state population, while n_7 is yet smaller. Checks using estimated but realistic $q_{6,1}$ and $q_{7,1}$ values, and measured areas for these bands with N_2 as a fill gas, show, e.g., a maximum[27] $n_6 = 1.9\%$ and $n_7 = 0.7\%$ of the total.

B. Relaxation Rates

The population data, as a function of fill gas pressure, are used in two ways. The first is a quantitative measurement of three vibrational transfer rates; the second, described in the Discussion, is aimed at a qualitative picture of the multi-quantum nature of the relaxation and requires mathematical modeling.

In order to extract relaxation rates from the vibrational population data, we calculate ratios of the $v'=4$ population S_4^* to the total B-state population S^*, and ratios of S_4^* to the populations in the adjacent levels, $v'=3$ and 5. This enables us to determine V', the total rate of transfer out of $v'=4$ and the rates $V'_{4,3}$ and $V'_{4,5}$ corresponding to single quantum transfer. The appropriate ratios among these three levels, and the sum S^*, are better determined at low fill gas pressure than ratios involving populations in $v'=0$, 1 and 2. Consequently these results yield directly quantitative rates, in contrast to those considered in the next section, which utilize all the data but require some modelling for their interpretation.

The data are first plotted versus A, according to Eq. (6), with $S_v^* = S_4^*$ and Q' set equal to zero. Thus we begin by explicitly neglecting the effects of back-transfer into $v'=4$. An obvious curvature is observed in each case, indicating that either or both of these phenomena must

---

27. *That is, the highest value attained by this pressure-dependent fraction.*

30

be taken into account. From other observations concerning the quench-ing,[28] together with the good fits obtained by the back-transfer correc-tions described immediately below, we are confident that the back-transfer is fully responsible for this curvature.

Using the initial (low-pressure) slope from these plots as a first estimate of V', the data are then plotted according to Eq. (7), with $v_f=3$ and 5. This permits a first determination of $V'_{4,3}$ and $V'_{4,5}$, again from initial slopes.

The assumption is then made that $V'_{3,4}=V'_{4,5}$ and $V'_{5,4}=V'_{4,3}$. This is quite reasonable for our use of these rates as correction terms, since (i) the anharmonicity in B-state S_2 is not large, and (ii) our modelling results indicate no strong dependence of the single-quantum transfer rates upon vibrational level. These values are then fed into Eq. (8) in order to redetermine V' with initial corrections for back transfer. The V' so obtained is used for a recycling through Eqs. (7) and (8), which produces a consistent set for V', $V'_{4,3}$ and $V'_{4,5}$.

The final transfer plots, i.e., the left-hand side of Eq. (8) vs. fill gas pressure, are shown in Fig. 5. The values of V' extracted from these plots, and the values for $V'_{4,3}$ and $V'_{4,5}$, are collected in Table II.

Unfortunately, final-state-specific rates, other than these two, cannot be reliably determined from the data. The low intensity of the $v'=6$ bands, at all pressures, and the problems mentioned earlier con-cerning n_2, preclude direct determinations of $V'_{4,6}$ and $V'_{4,2}$. While the values of n_1 are fairly well determined in general, a separation of the $V'_{4,1}$ rate from vibrational cascade through $v'=3$ and/or 2 requires the use of limiting slope data at quite low pressure; we feel the data is not of high enough precision in that region to yield a meaningful $V'_{4,1}$.

C. Vibrational Population Evolution

As the pressure of the fill gas is increased to successively higher values, the vibrational population distribution within $B^3\Sigma_u^-$ undergoes an evolution from a near-delta-function population of the initially pumped level to a near-thermal distribution over all levels. The fractional populations of vibrational levels $v'=0$ through $v'=5$ are plotted at several pressures of argon in Fig. 6. Each successive frame shows the steady-state population distribution after an approximately three-fold pressure increase over the preceding frame. The populations are calculated from transfer spectra like those shown in Fig. 1. For the two lowest pressures shown, the absence of values for $v'=0$, $v'=1$, or $v'=2$ result from the undetectability of transfer bands from these levels. (Although $v'=2$ probably has a population between those shown for $v'=1$ and $v'=3$ at 1.7 torr of argon, lack of a strong $v'=2$ band in a good viewing region prevented a direct calculation of its population.) The experiments exhibit a surprising similarity among the relaxation distributions found

---

28. *That quenching does not cause the curvature is discussed further below.*
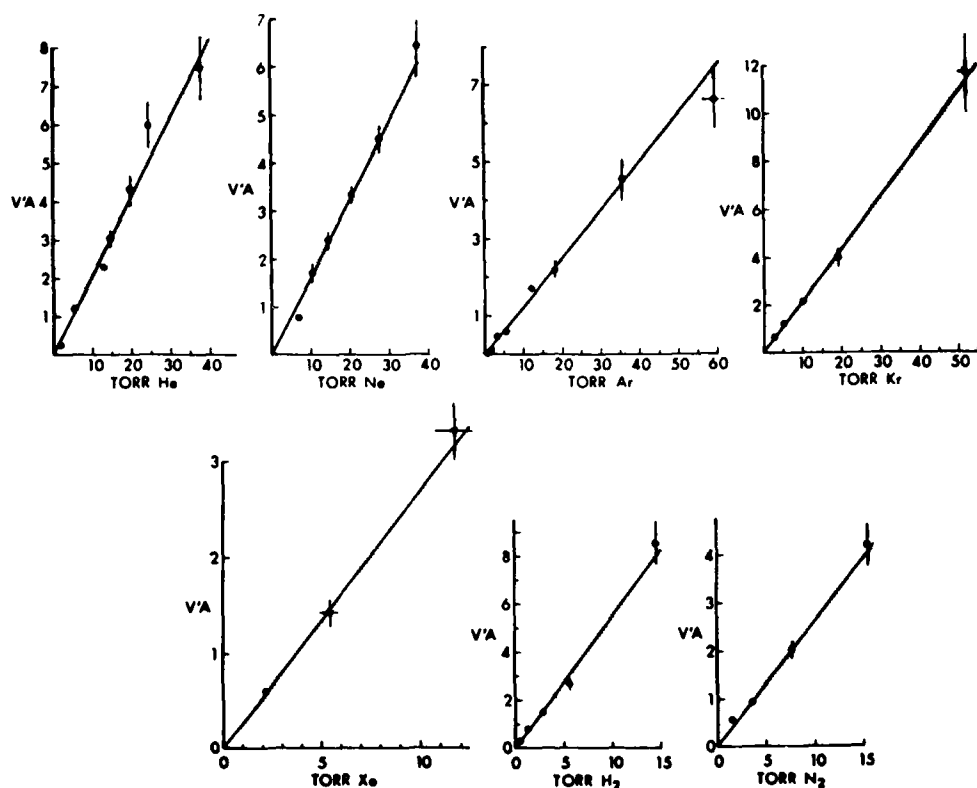
Figure 5. Plots of V'A (left-hand side of Eq. (8) vs. A, for each of
the gases studied. The error bars are estimates from the data. The
straight lines are the fits obtained with the quoted V' result, and the
shaded area corresponds to the limit using the error bars quoted also in
Table III.

32

TABLE II. VIBRATIONAL RELAXATION RATES AND CORRESPONDING CROSS-SECTIONS

GAS	Units: 10^{-10} cm^3 sec^{-1}			Units: 10^{-16} cm^2		
	V	$V_{4,3}$	$V_{4,5}$	σ	$\sigma_{4,3}$	$\sigma_{4,5}$
He	2.0±0.2	1.09±0.12	0.54±0.04	8.8±0.8	4.9±0.5	2.4±0.2
Ne	1.55±0.10	0.70±0.07	0.33±0.03	13.9±0.9	6.3±0.6	3.0±0.3
Ar	1.22±0.13	0.61±0.06	0.29±0.03	13.8±1.5	6.9±0.6	3.2±0.3
Kr	2.08±0.15	0.97±0.10	0.38±0.04	29±2	13.4±1.4	5.3±0.5
Xe	2.6±0.2	1.06±0.11	0.52±0.05	38±4	15.9±1.6	7.9±0.7
H_2	5.3±0.6	2.4±0.2	1.08±0.18	17±2	7.5±0.7	3.4±0.6
N_2	2.5±0.2	1.15±0.10	0.49±0.05	26±2	11.6±1.0	5.0±0.5

33

with He, Ne, Ar, Kr, Xe, H_2 or N_2 as the collision partner.

One can follow quite readily the thermalizing of the vibrational levels within $B^3\Sigma_u^-$. The population distribution first spreads and then piles up in the lowest vibrational levels with the v'=4 level always maintaining a larger population than its nearest neighbors, as is characteristic of a steady-state problem.[29] At the highest pressure shown, the steady-state distribution is nearly Boltzmann; the dashes in the last frame indicate equilibrium populations for an ensemble of harmonic oscillators with the S_2 excited state fundamental vibration frequency of 434 cm^{-1} in contact with a 900 K heat bath. Of course, there is no information about single collision dynamics by the time the system has reached such an advanced stage of relaxation. However, such a result further indicates that quenching is a much less likely process than vibrational relaxation.

Computer modelling of the relaxation process, and a comparison of the model's outputs with data such as that in Fig. 6, was performed to extract information on the effects of multi-quantum transfer and level-dependent transfer rates. These results will be treated in the discussion section.

D. Quench Rate Limits from Vibrational Relaxation Data

Information concerning quench rates for the rare gases, N_2 and H_2 as collision partners comes from three sources. The gentle slope of Fig. 3, at pressures of 10 torr and up, suggest quench rates for He and Ar of only about 1-2% of V'. The fact (see Fig. 6) that the upper-state population distribution evolves to a near-thermal distribution, a process requiring the occurrence of several transfer collisions before the S_2 molecules leave the excited state, demands that vibrational relaxation is significantly faster than quenching for all the gases.

The vibrational transfer plots constitute the third source. The observed curvature in the initial plots (Eq. (6) with Q'=0) could, *a priori*, be attributed to either quenching or back-transfer. However,

29. *It is perhaps conceptually easier to consider a time-domain experiment at fixed pressure, in which the exciting lamp is pulsed and the time evolution of the population is measured. In this, the pulsed, case, one would see an initial broadening of the narrow distribution with a movement of the peak of the population toward lower values of v' at increasing times, and, at very long times, a near thermal distribution. The steady-state experiment exhibits similar features as a function of pressure, though they are not quantitatively identical, due to the continuous source term in this case. The problem of vibrational relaxation with a pulsed source and a multi-level system is treated in E. W. Montroll and K. E. Shuler, J. Chem. Phys 26, 454 (1956), while that of rotational relaxation is discussed in R. Herman and K. E. Shuler, J. Chem. Phys. 29, 366 (1958). For the relationship between the pulsed and steady-state experiments, see T. Carrington, J. Chem. Phys. 35, 807 (1961).*
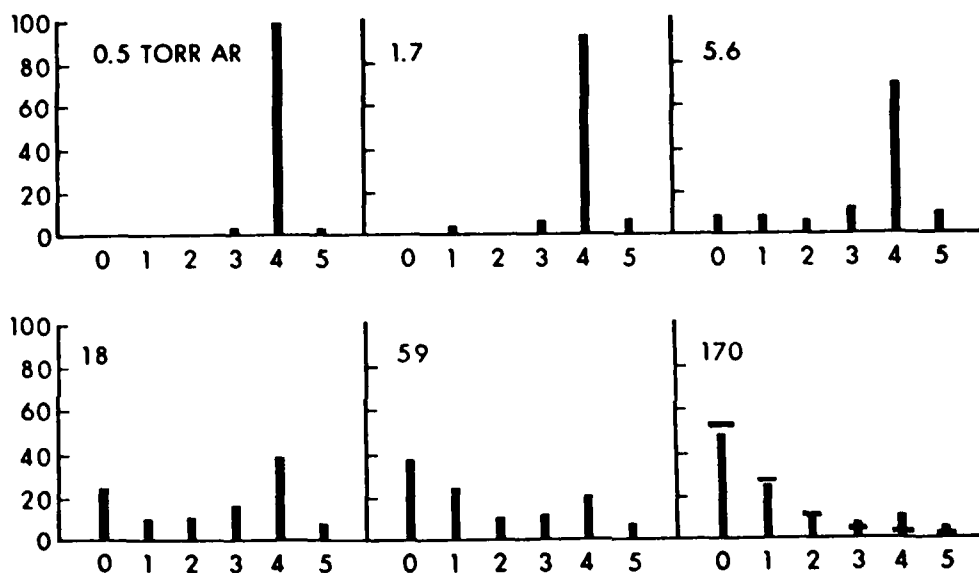
34

Figure 6. Fractional vibrational population in each v' level, at several Ar pressures as marked. The horizontal lines in the last plot are the Boltzmann fractions at the cell temperature.

35

the amount of curvature is much too great to be attributable to a quench rate as small as that established by the data discussed in the preceding paragraph. The transfer plots themselves (Figure 6), after incorporation of the back-transfer correction determined with independent S_3^* and S_5^* data and Eq. (7), are clean straight line fits to within the error bars of the data (with the exception of H_2; see below). The back-transfer correction thus fully accounts for the original curvature.

In fact the lack of residual curvature in the plots of Eq. (8), for all gases except H_2, prevents the determination of Q' from these data. Upper limits are set by replotting[9] using trial values for Q'. In this manner it is found that, except for Xe and H_2, the data are quite consistent with Q' < 0.1 V'. For Xe, an upper bound of 0.2 V' could be set by this procedure.

Only for H_2 did residual curvature remain after the back-transfer correction. Fits to Eq. (8) were made using trial non-zero values of Q' until the straight line plotted in Figure 6 resulted. The resulting value of Q' thus determined is $(1.0 \pm 0.5) \times 10^{-10}$ cm^3 sec^{-1}.

This quench rate is, however, not necessarily attributable to H_2 quenching collisions, but is more likely the result of quenching due to H_2S formed by reaction between H_2 and S_2. Studies[9] using H_2S directly as a fill gas show only small transfer even at several hundred torr. This shows that, as with $S_2(B) - S_2(X)$ collisions, quenching is the predominant fate of $S_2(B) - H_2S$ encounters.

Although thermodynamics favors a $[H_2S]/[H_2]$ ratio of 6.6 under our cell conditions and S_2 pressure, the kinetics are slow enough that only a small amount of H_2 is converted to H_2S during the actual measurement. Pressure data[9] taken before and after the experimental runs indicate that the quoted Q' was obtained in a mixture containing $\lesssim$ 14% H_2S. If all of the quenching is attributable to H_2S, this corresponds to a rate constant of 7 x 10^{-10} cm^3 sec^{-1}, or a cross section σ_Q = 80 $\AA^2$. The Hanle effect measurements[5] yielded for H_2S - used there directly as a fill gas - a coherence destruction cross section of 82 $\AA^2$. It is argued in Ref. 5 that σ_{cd} should be the same as σ_Q for S_2, SO_2 and H_2S. The agreement in this case, as with that of S_2, is close (here fortuitously so in view of error bar considerations).

E. Band Contours and Rotational Memory

Contours of transferred vibrational bands contain information about the possibility of the retention of the pre-collision rotational state distribution in the post-collision vibrational level. As mentioned earlier, the main rotational branches of the originally pumped level are easily resolved by the detector. Thus, if the rotational memory were quite strong, one would expect to see definite features, atop the overall contour of vibrationally transferred bands, which could then be attributed to emission from a single or a very few rotational levels having J' close

36

to that of the initially pumped level.

Since a secondary fluorescence series is simultaneously excited in v'=5 at about 1.5% of the intensity of the v'=4 series,[30] it was best to look for rotational memory in a strong v'=3 band. Of course, even if complete rotational information were transferred to this adjacent vibrational level, a v'=3 band would appear more rotationally relaxed than a v'=4 band because the v'=3 state would have inherited a partially relaxed rotational distribution from the v'=4 band and would have experi- enced further relaxation on its own. Even so, we have never seen, with any gas, line-type features attributable to complete retention. The sensitivity of the detection apparatus and the cleanliness of the spectrum from other interferences would clearly reveal the peaks down to at least 20% of their anticipated size were the rotational memory perfect.

While a perfect rotational memory is a limiting case and not really expected to occur, evidence of partial memory would be revealed in the contour of the transferred bands. We do observe a non-Boltzmann distri- bution in the v'=3 bands after collisions of S_2 with H_2. The over abun- dance of high-J emitters give a rounded looking band without a strongly developed head. However, we were not able to conclude whether the distri- bution was skewed to either higher or lower J-values than the original J'=41. H_2 is the best gas to use when looking for rotational memory since the σ_R/σ_V ratio is small (see below), rotational relaxation within v'=4 occurs mainly by small changes in J (see next section) so that the initial J-distribution does not spread quickly, and the slight quenching by H_2S also favors observing the effect. With all the other gases we could not definitely claim to have made even this qualitative observation of strongly nonthermal transferred bands. We attribute this to a lack of detection sensitivity and not necessarily to a total lack of rotational memory.

VI. ROTATIONAL TRANSFER

Using the same wavelength resolution as for the vibrational transfer experiments, measurements of the total rate of rotational relaxation from the initially pumped N'=40, J'=41 level were made. For this total rota- tional relaxation rate, post-collision states are specified only as different rotational (or fine structure) levels within v'=4. For a specification of final states and a determination of state-to-state rates, intensity measurements with a higher resolution are required; these are described in a subsequent paper.[4] As in the preceding section, data analysis first involves extracting populations from intensity measure- ments and then the use of this information to calculate relaxation rates. Finally, band contours are examined for trends in the degree of multi- quantum transfer among the different collision partners.

---

30. *Excited by the Zn 303.6 nm line.*

A. Population Determinations

The data analysis, Eq. (9), requires the ratio of the population of the initially pumped rotational state, S_J^*, to the total population within $v'=4$, S_v^*. The latter was determined as in the vibrational transfer experiments, using Eq. (11) and the areas of the $v'=4$ bands having $v'' = 2, 3, 6, 7$ and 10. Because some vibrational relaxation occurs within the pressure range used here, small corrections were necessary to account for overlapping $v'=2$ bands.

A measure of S_J^* was obtained from measurements of the height of the R_1, and the blended P_1 and $^P R_{13}$ lines of the initial rotational level at a series of foreign gas pressures together with a calibration measurement at zero pressure. Since rotational relaxation may appear as a slight broadening of these fluorescence lines, causing a measurement of the area of the lines to include intensity from rotationally transferred levels, a height measurement is more indicative of the true population of the initially pumped rotation state. Heights were measured as the distance from the peak of a line to a baseline estimated from the amount of signal lying to the high and low wavelength sides of the nontransferred lines (i.e., the baseline was not the zero-intensity baseline as used for vibration measurements). While some rotationally transferred levels may still emit fluorescence contributing to the height of the lines, such contamination should not be large. Indeed, measurements based on higher resolution spectra[4] always confirmed the measurements made at this lower resolution to within a random 10% variation. The calibration consisted of a measurement of the height and area of these lines for each band, in the absence of foreign gas. This provided the conversion factors connecting the peak height measurements of S_J^* and the band area measurements of S_v^*. The slit width settings on the monochromator were untouched (not merely reset) from one gas to another so that good statistics resulted from averaging together the calibration scans run for each gas.

The ratio S_v^*/S_J^* was calculated separately for each band used at each pressure of the collision partner. Good agreement among all five bands was found, indicating no systematic errors in our analysis procedure and the absence of any effects due to reabsorption of the fluorescence. Also, since there seemed to be no systematic difference between the areas computed on the basis of the height of the R_1 line and the height of the P_1 and $^R P_{13}$ combination, the average of the values was used.

B. Relaxation Rates

The data are analyzed according to Eq. (9), again with the quenching rates Q' set equal to zero (except for H_2) and using the values of V' determined above. Initial plots neglecting the effects of vibrational back-transfer showed a noticeable curvature. The back-transfer term is calculated at each pressure using the previously determined rates $V'_{3,4}$ and $V'_{5,4}$ and the previously measured population ratios S_3^*/S_J^* and

38

S_5^*/S_J^*; it is not fitted to the present data. Hence, the only parameter extracted from Eq. (9) is R'. Plots of the data and the range of the predicted values are shown in Figure 7, and the results are presented in Table III.

The major causes of the uncertainty at the high pressures is the uncertainty in V', and some uncertainty in the experimental ratio S_v^*/S_J^*. As a gauge of the latter, we consider the standard deviation on the average of the 10 determinations (5 bands each with the R_1 and the $P_1-^{Rp}P_{13}$ lines). At 0.77 torr, the deviation is 5% while at 10.4 torr it is 9%.[13] This lower uncertainty at lower pressures, a general trend, is however magnified by the near-unity ratio of S_4^*/S_J^* at low pressures.

Rotational back-transfer has not been included in the analysis, and the lack of any downward curvature in the plots of Figure 7 indicates that it is unimportant at these pressures. This is consistent with expectations. Although the rotational levels are much more closely spaced, compared with the vibrational levels, the strong multi-quantum flavor of the rotational relaxation[4] spreads the population out over such a large number of levels that transfer back into the initially pumped one is relatively improbable. In addition, the competing vibrational transfer inhibits the likelihood of rotational back transfer.

C. Band Contours and Multi-Quantum Transfer

As mentioned earlier, the spectrometer slit width was untouched between spectral scans with different collision partner gases. The reproducible bandwidth obtained with this procedure allowed a comparison of the $v'=4$ band shapes as a function of inert gas. In particular, we compared band shapes produced by different gases at pressures which caused nearly identical degrees of rotational relaxation.

In Figure 8 is shown a comparison of the contour of the (4,2) band, for each collision partner at a pressure such that about 30% of the $v'=4$ population is that of rotationally transferred molecules. The actual values are listed in Table IV. For these scans, vibrational back transfer is insignificant.

The lighter collision partners show more emission from the rotationally transferred molecules occurring in the region of the fluorescence lines from $N'=40$, $J'=41$. This corresponds to rotational levels in the general vicinity of these quantum numbers. In contrast, the heavier gases show a spreading of the emission over a larger wavelength range. For N_2 and Kr, and especially for Xe, a marked band head is noticeable; this corresponds to emission from levels with much lower J'. Since the degree of total rotational relaxation is the same in each case, one may immediately draw the qualitative conclusion that the average change in J per collision is greater for the heavier collision partners, while small mass of the collision partner favors a small change in J. These inferences from the band contour examinations are borne out by the state-to-state rates

39

TABLE III. ROTATIONAL RELAXATION RATES AND CORRESPONDING CROSS SECTIONS

GAS	$R(10^{-10} \text{ cm}^3 \text{ sec}^{-1})$	$\sigma(10^{-16} \text{ cm}^2)$
He	8.2 ± 1.0	37 ± 4
Ne	6.2 ± 0.6	56 ± 5
Ar	5.7 ± 0.6	65 ± 6
Kr	6.4 ± 0.6	88 ± 8
Xe	4.8 ± 0.5	72 ± 7
H_2	15 ± 2	49 ± 7
N_2	7.9 ± 0.8	79 ± 8
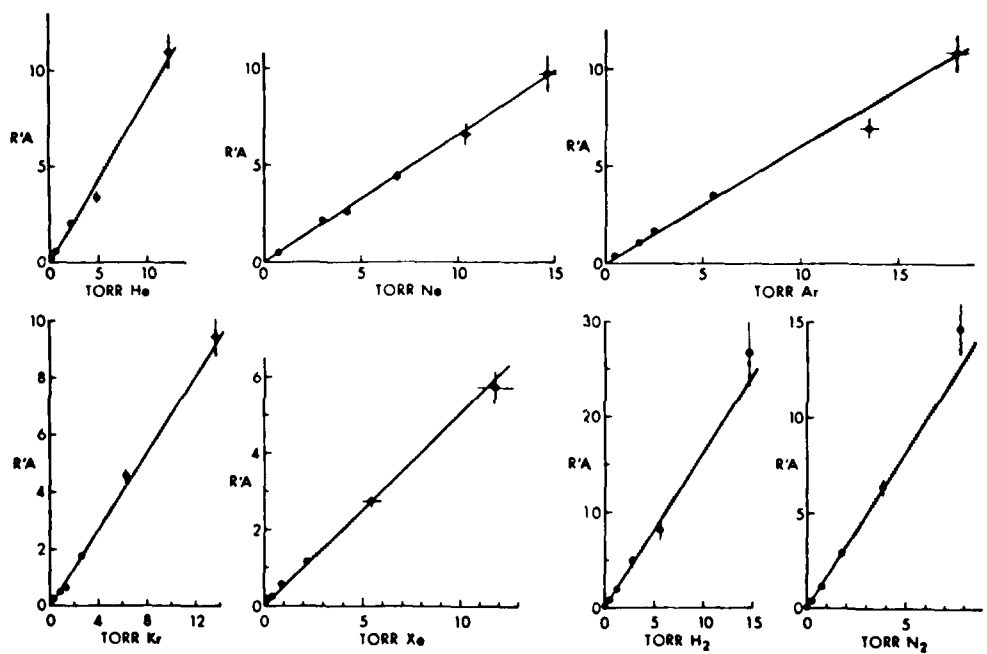
Figure 7. R'A plots (left-hand side of Eq. (9) vs. A for each collision
partner. As in Fig. 5, error bars are estimates from the experimental
data, and the straight line and shaded areas are predictions using the
quoted results for R' and its error limits.

41
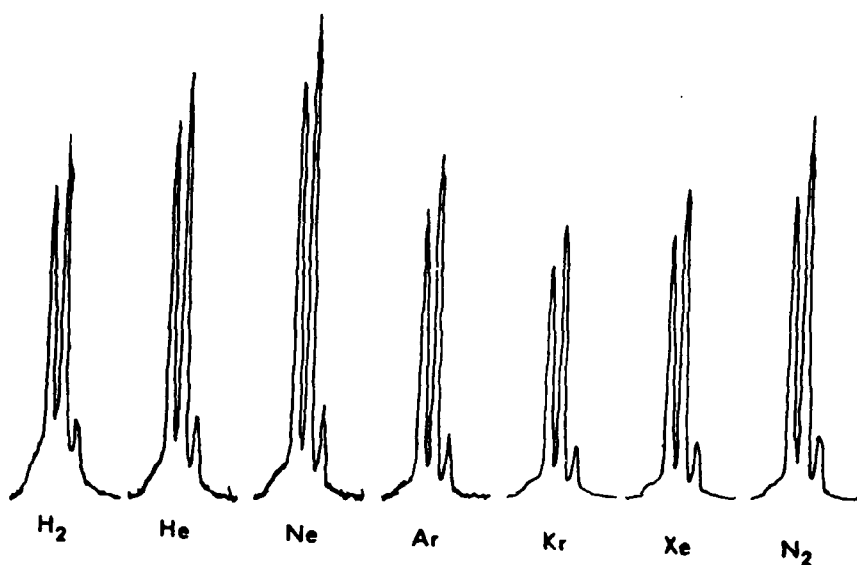
Figure 8. Scans of the (4,2) band for each collision partner at similar degrees of rotational relaxation, showing the difference in rotational contours: in the lighter gases, the relaxation is more to rotational levels in the neighborhood of the initially pumped level, while for the heavier gases the rotationally relaxed molecules are spread out over a larger range of J'. The pressures and actual fractions of rotational relaxation for each scan are given in Table IV.

TABLE IV. RELAXATION PARAMETERS PERTINENT TO FIGURE 8

GAS	PRESSURE (torr)	FRACTION OF ROTATIONAL RELAXATION $(1 - S_J^*/S_4^*)$
He	0.66	0.34
Ne	0.76	0.29
Ar	0.54	0.26
Kr	0.89	0.29
Xe	0.90	0.29
H_2	1.28	0.37
N_2	0.55	0.23

reported in Reference 4.

VII. DISCUSSION

Quenching has been seen to be the most probable outcome of an encounter of B-state S_2 with ground state S_2. The fact that S_4 is a stable molecular entity suggests that S_2-S_2 collisions could well be long enough lived to lead to a fairly equal sharing of the total energy between the parting pairs of diatomics.

On the other hand, quenching is a relatively unlikely process when $B^3 \Sigma_u^- S_2$ collides with a rare gas or N_2 (or, we suspect, H_2). While an upper limit for Q' of 0.1 V' can be estimated by using the vibrational transfer data, the measurements of total fluorescence intensity with increasing pressures of He and Ar suggest a significantly smaller Q', of the order of 0.02 V'. The primary result of a collision, then, is to transfer the S_2 into another energy level of the B-state. Since quenching is small, we can follow the changes in population from that of the single initially pumped level to that of a nearly thermal distribution over rotational and vibrational modes.

In this discussion section, we examine some discernible trends in the cross sections for total rotational and vibrational transfer, and we consider some aspects of state-to-state vibrational transfer, chiefly via a model of the population evolution. We conclude with a brief comparison of the present results to prior studies on $B^3 \Sigma_u^- S_2$.

A. Trends in the Cross-Sections

The cross sections σ_V and σ_R for total vibrational and rotational transfer are all relatively large, of the order of gas kinetic values. This is rather common (though not universal) for relaxation cross sections within excited electronic states, and has been attributed to the high polarizability of excited states. While the present results bear no direct evidence on this point, they do show a smooth increase in cross section with increasing mass of the collision partner.

In Figure 9 are plotted the cross sections as a function of the square root of μ, the reduced mass of the collision pair. In general, both σ_R and σ_V increase smoothly with $\mu^{1/2}$. For σ_V, such behavior might be anticipated by a picture of the transfer process occurring during a relatively brief encounter, whose efficiency increases as the collision duration (which is proportional to $\mu^{1/2}$) approaches the vibrational period.

The relative efficiency of the diatomics vs. the monatomics, for both σ_V and σ_R, also suggests a brief collision. While H_2 and N_2 have somewhat larger cross sections than a rare gas of equivalent μ, the difference is much smaller than would be expected from a statistical partitioning of the energy into the available internal levels of the diatomic.
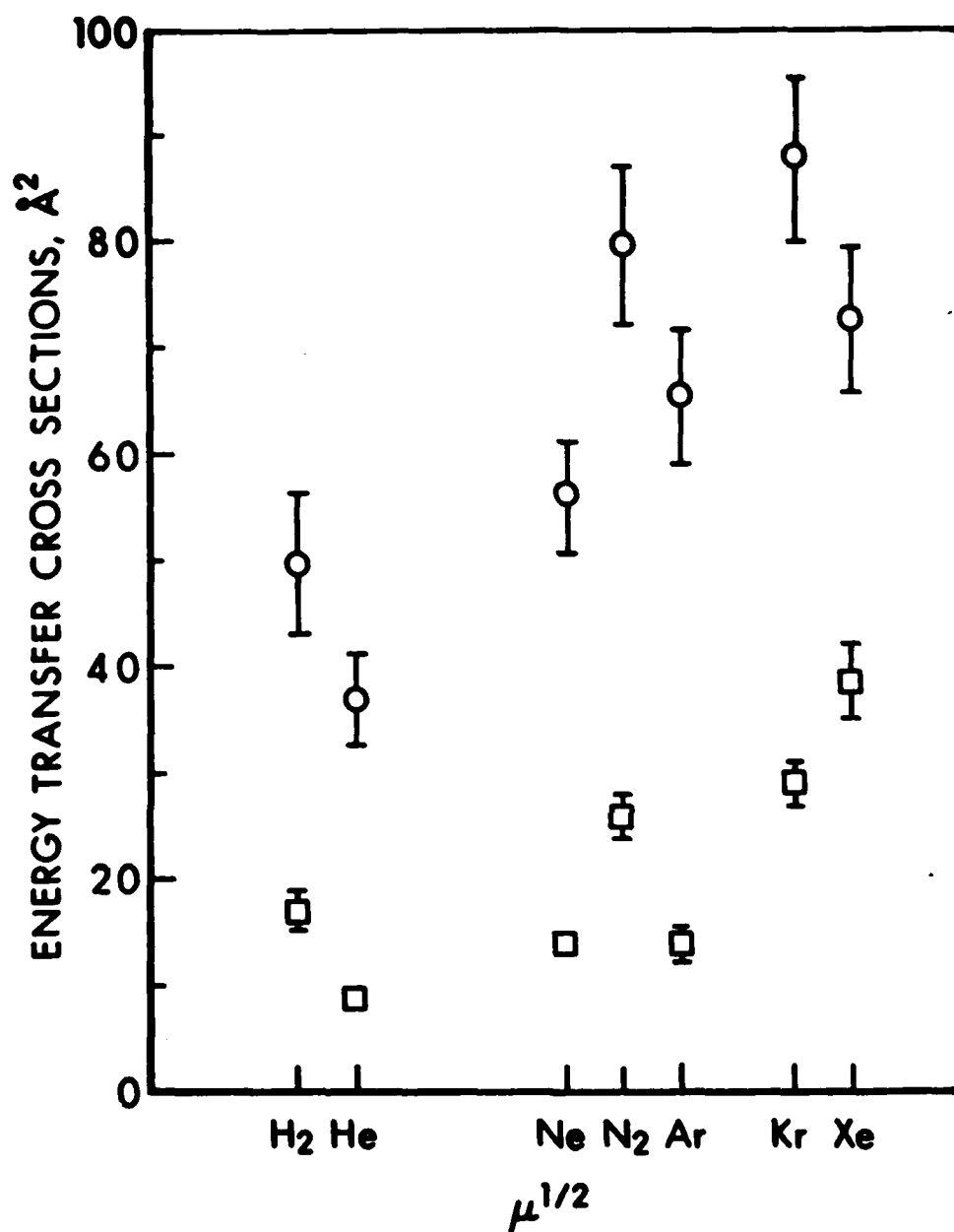
44

Figure 9. Vibrational (squares) and rotational (circles) transfer cross sections plotted vs. the square root of the reduced mass of the S_2 and the collision partner indicated.

45

A simple interpretation of the smooth variation of σ_R with $\mu^{1/2}$ is also supportive of such a view. Steinfeld,[14] observing similar behavior in I_2, noted that the cross-sections may reflect simply the amount of rotational energy available in a collision. If it is assumed that the average impact parameter b does not change drastically upon going from one gas to another, then the amount of angular momentum L available in a collision varies as the square root of the reduced mass of the collision pair.

$$L = \mu v b \propto \mu/\mu^{1/2} = \mu^{1/2},$$

where v is the mean relative velocity. Such a simple interpretation may be true only when the interaction period is shorter than the rotational period of the molecule. For example, Bergmann, et al.[31] have studied the J-dependence of cross-sections for $\Delta J = \pm 1$ transfers (the major constituent of the total rotational transfer cross-section in their case) in $B^1\Pi_u$ Na_2, excited by argon ion laser lines. They find a mass dependence for σ_R at small J qualitatively similar to the one found here. However, at high J the σ_R for collisions of the heavier rare gases with Na_2 is lowered, producing little variation in σ_R with mass. They explain such behavior by saying that the faster rotation rate presents a more spherical potential to the perturber when the period of rotation becomes less than the interaction time. The interaction remains anisotropic for the lighter gases since they quickly zip past the diatomic sodium. In fact, the slight decrease in σ_R which we find for Xe compared to Kr could be a manifestation of this rotational averaging, and were one to initially excite near N'=60, this idea could be tested.

B. Vibrational Transfer Rates

The fact that the sum of $V'_{4,5}$ and $V'_{4,3}$ is less than V' for each collision partner constitutes a strong argument for the presence of multi-quantum vibrational transfer. Here we examine, via computer modelling of the data represented in Figure 6, some possible assumptions about relative rates.

Before that, however, we note the similarity, for all the collision partners studied, of the fraction of the total vibrational transfer rate constituted by $|\Delta v| = 1$ transfers, and the remarkable constancy of the ratio $V'_{4,5}/V'_{4,3}$ (see Table V). This has the implication that the phenomenological mechanism describing relative rates is similar for each gas, so that the conclusions below pertain to all. In addition, there is here a suggestion of a similar collisional mechanism for each gas, in accord with the views of the preceding section.

31. K. Bergmann, W. Demtroder, M. Stock and G. Vogl, J. Phys. B 7, 2036 (1974).

TABLE V. RELAXATION RATE RATIOS

GAS	$V_{4,3}/V$	$V_{4,5}/V$	$(V_{4,3}+V_{4,5})/V$	$V_{4,5}/V_{4,3}$	R/V
He	0.56±0.08	0.28±0.03	0.83±0.12	0.50	4.2±0.6
Ne	0.45±0.05	0.22±0.02	0.67±0.08	0.47	4.0±0.5
Ar	0.50±0.07	0.23±0.04	0.73±0.11	0.48	4.7±0.7
Kr	0.47±0.06	0.18±0.02	0.65±0.08	0.39	3.1±0.4
Xe	0.41±0.06	0.20±0.03	0.62±0.08	0.49	1.9±0.3
H_2	0.45±0.07	0.21±0.04	0.65±0.11	0.45	2.9±0.5
N_2	0.46±0.05	0.20±0.03	0.65±0.08	0.43	3.1±0.4
Average	0.47	0.22	0.69	0.46	-

47

In addition, some information on the level dependence of the $\Delta v = -1$ rates is available from the experiments together with the invocation of detailed balancing.

$$\sigma_{5,4}/\sigma_{4,3} = (\sigma_{4,5}/\sigma_{4,3})(\sigma_{5,4}/\sigma_{4,5}).$$

The application of detailed balancing to obtain the second ratio on the right hand side must be approached with some caution. The vibrational rates we measure are those of a single initial rotational level undergoing vibrational transfer into a particular final rotational distribution. We use for the $\sigma_{5,4}/\sigma_{4,5}$ ratio, however, the value $\exp[(E_5-E_4)/kT]$ which is appropriate to thermal distributions in each vibrational level. We justify this by noting that our initial value $J'=41$ is close to the most probable value of J' (*viz.*, 37) for a thermal distribution at 873 K. The rotational contour studies (Figure 8) indicate a final state distribution somewhere between rotational memory and a thermal distribution, which are similar for the current purposes. In particular, isoenergetic transfer (to $N' \sim 0$ in $v'=5$), for which this detailed balancing expression would be wholly inappropriate, does not predominantly occur.

We use the average value $\sigma_{4,5}/\sigma_{4,3} = 0.46$ to obtain $\sigma_{5,4}/\sigma_{4,3} = 0.88$.

Computer modeling of the relaxation of the initial vibrational distribution was performed in order to gauge the effect of multi-quantum and vibration level-dependent transfer rates on the relaxing distribution. These studies were qualitative, in the sense that exact agreement with experiment was not expected; rather, matching the observed relaxation pattern was sought by varying the rate constants. The experiments show a surprising agreement between the relaxing distributions found with He, Ne, Ar, Kr, Xe, H_2, or N_2 as collision partner; and so the modeled results are compared to one experimental relaxation pattern.

The model calculation solves for the steady-state populations of twelve vibrational levels. It is constrained to the initial condition that when all transfer rates are zero (i.e., at zero pressure), all of the population resides in $v=4$. Given as input are the rates of transfer of population between any two levels. While there are only ten bound vibrational levels in the B-state, and population data for only six of these, the calculation involves a larger number for mathematical convenience. This prevents any pileup of population in the highest level included in the model, and permits a more general set of relative rates to be used as input. The calculation involves solving twelve linearly independent equations in twelve unknowns by matrix inversion.

The model, carried out to simulate a series of steady-state experiments, confirms the general features of the development of the vibrational

distribution as shown in Figure 6, namely that the initial distribution first broadens about v=4 and then population piles up in the lower vibrational levels until a thermal condition exists. Variation of relaxation rate constants and the relative importance of multiquantum events do not alter these gross features of the relaxing distribution. However, noticeable differences (compared to experiment), dependent on the relative rates chosen as input, do exist for the rate of increase of the lower vibrational populations relative to the population decrease of v=4.

Of course, with so many rate constants to specify, the starting point is to use only "reasonable" rate constants, avoiding unnecessarily complicated schemes. The first model limited vibrational transfers to $\Delta v=\pm1$ events only and took the up-transfer rates to be independent of vibrational level (the down-transfer rates being determined by detailed balancing). Such a model clearly failed to mimic the experimental findings. The v=3 population attained too large a population while the v=0 and v=1 levels did not grow in population fast enough. Still limiting transfers to $\Delta v=\pm1$, one would need to have the lower vibrational levels relax very much faster than the upper ones for the model to exhibit the proper trends. Nonetheless, we could never satisfactorily match the experimental data under this constraint.

One can more quickly build up the population of the lower lying vibrational levels by allowing multi-quantum transitions. This also leads to a slower build up of v=3 for a given decrease in v=4. The addition of $\Delta v=\pm2$ improves agreement with experiment, but still fails to simulate the data unless the $\Delta v=+2$ rate is significantly greater than the $\Delta v=+1$ rate, which is physically unrealistic. However, inclusion of a $\Delta v=+3$ rate, of one-half the $\Delta v=+2$ rate (which in turn is one-half the $\Delta v=+1$ rate) for a given level, yields quite good agreement with experiment. Adding a $\Delta v=+4$ rate of one-half the $\Delta v=+3$ rate produces even slightly better agreement with experiment. Thus, if vibrational transfer rates are assumed independent of v, $\Delta v=\pm3$ transfer must be invoked to explain the experimental results and including $\Delta v=\pm4$ transfers produces even further improvement. Higher-order multiquantum transitions were not modeled since they would produce negligible changes in the modeled distributions.

We note two direct comparisons of the model's final input figures with experimental results. The experimental $\Delta v=+1/\Delta v=-1$ ratio is 0.46, on the average, while the model uses 0.50; $\Delta v=\pm1$ transfers constitute 69% of the total measured vibrational transfer rate while the corresponding figure for the model is 59%.

We conclude from this phase of the study the qualitative result that significant rates of multiquantum transfer are necessary to explain the data exemplified in Figure 6. While this is unambiguous, the data is not of sufficient overall quality to warrant extraction of quantitative individual V_{4,v_f} rates for v_f other than 3 and 5.

49

A useful viewpoint may be gained by examination of the model rate constants used in our master equation approach, in terms of information theoretic analysis.[32] We found satisfactory agreement (we make no claims as to uniqueness) using rates independent of v_i, and scaled by successive factors of one half. In terms of the rate constants $k(v_i \rightarrow v_f) \equiv k(\Delta v)$, this may be expressed as

$$k(1) = 2k(2) = 4k(3) = 8k(4) \; , \tag{12}$$

For a series of rate constants of this nature, the surprisal $I_{\Delta v}$ is defined in terms of the ratio of $k(\Delta v)$ to the 'prior' rate constant $k^0(\Delta v)$:

$$I_{\Delta v} = - \ell n [k(\Delta v)/k^0(\Delta v)] \; .$$

$k^0(\Delta v)$ is the rate constant expected were the rates to be determined solely on the basis of statistics; that is, it represents the density of final states available to the system for a collision in which a change Δv occurs. Hence a non-zero $I_{\Delta v}$ reflects a 'dynamic bias' in the collisional encounter, yielding a measure of the degree to which the collision dynamics - not just statistics - influence the outcome of the collision. It has been found[32] that a large number of collisional processes have surprisals which are linear functions of the amount of energy transferred. In terms of the surprisal parameter λ,

$$I_{\Delta v} = \text{const} + \lambda [E(v_i) - E(v_f)/kT], \tag{13}$$

where T is the temperature of the heat bath into which the vibrational energy is transferred.

We have calculated the $k^0(\Delta v)$ from the prescription in Rubinson and Steinfeld,[33] using anharmonic oscillator to represent the S_2 vibration. From these and the set of model rate constants of Eq. (12), we make the surprisal plot of Eq. (13). It is linear with a slope $\lambda=1.3$. Thus our model set of $k(\Delta v)$ is in neither the statistical limit ($\lambda=0$) nor the adiabatic limit ($\lambda \gg 1$). The "effective width" of a transition,[34]

32. R. D. Levine and R. B. Bernstein, Acc. Chem. Res. 7, 393 (1974).

33. M. Rubinson and J. I. Steinfeld, Chem. Phys. 4, 467 (1974).

34. I. Procaccia and R. D. Levine, J. Chem. Phys. 63, 4261 (1975).

a measure of the amount of energy transferred in a collision in which some transition occurs, is $kT/\lambda = 470$ cm^{-1}, a bit larger than the single quantum spacing of 434 cm^{-1}. The value of λ obtained is in accord with our earlier and independent arguments about the duration of the collisional encounter, which were based on the variation of σ_v with mass of the collision partner.

Other sets of rate constants scaled by a constant ratio, as in Eq. (12) where the ratio is 2, have also been tried in the model. We can reproduce the qualitative features of the data with a ratio between 1.5 and 3, although the models with these limits are clearly inferior to the set in Eq. (12). These limits would yield values of λ of 0.9 and 2.0 respectively.

We reemphasize that $\lambda=1.3$ is not a surprisal parameter extracted directly from our experimental data, which we feel is unwarranted. Rather, it is a surprisal parameter descriptive of our model rates in Eq. (12), which are in turn consistent with the data. (We have not explored sets of rates with a non-constant ratio, and thus Eq. (12) is probably not unique, only adequate.) Nonetheless, this λ provides a useful gauge, and categorization, of the vibrational energy transfer within $B^3\Sigma_u^-$ S_2.

C. Comparison with Other Investigations

The earliest studies of energy transfer in selectively excited S_2 have already been alluded to in the introduction. Rompe's findings[1,2] that transfer dominated over quenching, and that $\Delta v=-2$ changes occurred though more slowly than $\Delta v=-1$, for collisions with He, Ne or N_2, are well confirmed by the present work, as is Heil's[2] result that ground state S_2 efficiently quenches excited S_2.

Heil's foreign gas quenching measurements were designed much like our own initial attempts to obtain these quantities, except for slight differences in handling the sulfur. His results for He quenching of the fluorescence correspond to an upper limit $\sigma_Q < 0.6$ Å^2, which is slightly higher than the value suggested by the gentle slope of Figure 3. What puzzles us greatly is why he did not observe the sharp decrease in fluorescence intensity at low He pressures.

Durand[3] employed the Mg II lines at 292.8 and 293.7 nm to excite fluorescence in S_2. These lines fall in the region of the (8,1) and (6,0) bands; on the basis of the observation of an anti-Stokes fluorescence term - the (8,0) band - he quite reasonably assigns the excitation to v'=8. In actuality however, his excitation is an admixture of v'=8 and 6. An examination[9] of his relative band intensities shows that the dominant excitation is to v'=6.

Durand finds a sizeable decrease in fluorescence intensity upon addition of each of the rare gases. This he attributes to quenching,

and suggests collision-induced predissociation as the explanation for the large cross sections he obtains. This mechanism seems tenuous, in view of the fact that v'=6 is some 1500 cm^{-1} from the predissociation limit. Rather, we feel that he may have been observing the same kind of sharp decrease in intensity as we have seen. While his experimental setup is quite similar to ours, he operates at much higher S_2 pressures (1.1 torr) than do we, so that the hydrodynamic limit should be applicable to his experiments. Thus, if he is observing the same kind of fluorescence decrease as we did, one would expect it to be of somewhat smaller magnitude.

The quenching rates which Durand gives are larger, by a factor of six, than our upper limits from the vibrational energy transfer plots, and thus a factor of sixty larger than those corresponding to the gentle slope of Figure 3. We feel his values are not correct.

While Durand also observes and analyzes vibrational energy transfer data, a meaningful comparison is difficult. Suffice it to say that his transfer results are explicable only by transfer rates of the general size found here, that is, of gas kinetic size.

Fair and Thrush[35] have made measurements of the chemiluminescence produced by S-atom recombination in a discharge flow system containing H, H_2S and Ar. Their results for Ar quenching correspond to a rate constant 2.5×10^{-10} cm^3 sec^{-1}, twice as large as our Ar vibrational transfer rate. This is completely incompatible with our results although we do not know why. It should be noted that Fair and Thrush observe primarily much higher vibrational levels than we study here, but even for high v' it seems large. While they remark on the fact that it is a large value, they also note that systematic errors, if present, would likely make their reported value low.

McGee and Weston[16] have made lifetime measurements of S_2 fluorescence following excitation by a broadband (9.6 nm) pulsed source; they excite a mixture of vibrational levels with a most probable value near v'=7.[11] Their reported self-quenching cross section of 81 Å^2 is much smaller than our value of 180 Å^2. Even though they and we work with different vibrational levels, that is not likely to be the cause of the discrepancy, since Hanle effect measurements[5] point to an even larger $Q_s{}'$ for v'=9. We can find no reason why these measurements and ours should disagree. On the other hand, we take comfort in the agreement between our two independent methods - intensity of fluorescence and Hanle effect broadening - for obtaining $Q_s{}'$. The only systematic error which would affect each of these determinations in the same quantitative way is the manner in which we extract the actual S_2 pressure from the thermodynamic data and the cell flow conditions. In turn, we have confidence in this procedure from the absorption measurements, as described earlier.

35. R. W. Fair and B. A. Thrush, Trans. Far. Soc 65, 1208 (1969).

ACKNOWLEDGMENTS

REFERENCES

1. R. Rompe, Z. Phys. $\underline{65}$, 404 (1930).

2. O. Heil, Z. Phys. $\underline{74}$, 18 (1932).

3. E. Durand, J. Chem. Phys. $\underline{8}$, 46 (1940).

4. T. A. Caughey and D. R. Crosley, to be published.

5. T. A. Caughey and D. R. Crosley, Chem. Phys. $\underline{20}$, 467 (1977).

6. S. R. Leone and K. G. Kosnik, Appl. Phys. Lett. $\underline{30}$, 346 (1977).

7. P. Scott, Xonics, Inc., private communication, 1977.

8. C. H. Muller II, K. Schofield, M. Steinfeld and H. P. Broida, Bull. Amer. Phys. Soc. $\underline{23}$, 74 (1978).

9. T. A. Caughey, Ph.D. Thesis, University of Wisconsin, 1977.

10. Efficient coupling was difficult to achieve with this lamp, and it was necessary to force-air cool the connecting cable to prevent it from melting.

11. K. A. Meyer, Ph.D. Thesis, University of Wisconsin, 1976.

12. K. A. Meyer and D. R. Crosley, J. Chem. Phys. $\underline{59}$, 1933 (1973).

13. K. A. Meyer and D. R. Crosley, Can. J. Phys. $\underline{51}$, 2119 (1973). The spectroscopic notation is as follows, with $\Delta J = J'-J''$ and $\Delta N = N'-N''$: R_1, $\Delta J=\Delta N=1$; P_1, $\Delta J=\Delta N=-1$; $^{P}R_{13}$, $\Delta J=-1$, $\Delta N=1$; $^{N}P_{13}$, $\Delta J=-1$, $\Delta N=-3$.

14. J. I. Steinfeld and W. Klemperer, J. Chem. Phys. $\underline{42}$, 3475 (1965).

15. T. A. Caughey, K. A. Meyer and D. R. Crosley, to be published.

16. T. H. McGee and R. E. Weston Jr., Chem. Phys. Lett. $\underline{47}$, 352 (1977).

17. This procedure allows for a dark current correction and avoids changes in the quartz window transmission with temperature.

18. 10 cm of 0.23N $cuSO_4$ plus a glass filter similar to Corning 7-60, yielding a passband between 320 and 400 nm.

19. A. N. Nesmainov, Vapor Pressure of the Chemical Elements, (Elsevier, New York), 1963.

20. K. A. Meyer and D. R. Crosley, J. Chem. Phys $\underline{59}$, 3153 (1973).

21. A. C. G. Mitchell and M. W. Zemansky, Resonance Radiation and Excited Atoms, (Cambridge Univ. Press, Cambridge) 1961.

22. It could be argued that the presence of non-zero self-transfer, together with a lack of coherence retention for S_2-S_2 collisions, is what causes the σ_{cd} of Ref. 4 to be slightly greater than the σ_Q measured here. While the difference between them is about the right size, the two values overlap to within their error bars and such an interpretation is tenuous.

23. R. W. B. Pearse and A. G. Gaydon, The Identification of Molecular Spectra, 3rd Ed. (Chapman and Hall, London, 1965).

24. A. Fowler and W. M. Vaidya, Proc. Roy. Soc. A 132, 310 (1931).

25. The notation following implicity labels each area by the (v',v") band forming the dominant contribution.

26. G. D. Brabson and R. L. Volkmar, J. Chem. Phys 58, 3209 (1973); G. D. Brabson, private communication (1973).

27. That is, the highest value attained by this pressure-dependent fraction.

28. That quenching does not cause the curvature is discussed further below.

29. It is perhaps conceptually easier to consider a time-domain experiment at fixed pressure in which the exciting lamp is pulsed and the time evolution of the population is measured. In this, the pulsed, case, one would see an initial broadening of the narrow distribution with a movement of the peak of the population toward lower values of v' at increasing times, and, at very long times, a near thermal distribution. The steady-state experiment exhibits similar features as a function of pressure, though they are not quantitatively identical, due to the continuous source term in this case. The problem of vibrational relaxation with a pulsed source and a multi-level system is treated in E. W. Montroll and K. E. Shuler, J. Chem. Phys 26, 454 (1956), while that of rotational relaxation is discussed in R. Herman and K. E. Shuler, J. Chem. Phys. 29, 366 (1958). For the relationship between the pulsed and steady-state experiments, see T. Carrington, J. Chem. Phys. 35, 807 (1961).

30. Excited by the Zn 303.6 nm line.

31. K. Bergmann, W. Demtroder, M. Stock and G. Vogl, J. Phys. B 7, 2036 (1974).

32. R. D. Levine and R. B. Bernstein, Acc. Chem. Res. 7, 393 (1974).

33. M. Rubinson and J. I. Steinfeld, Chem. Phys. 4, 467 (1974).

34. Procaccia and R. D. Levine, J. Chem. Phys. 63, 4261 (1975).

35. R. W. Fair and B. A. Thrush, Trans. Far. Soc 65, 1208 (1969).

DISTRIBUTION LIST

No. of Copies	Organization	No. of Copies	Organization

12 **Administrator**
Defense Technical Info Center
ATTN: **DTIC-DDA**
Cameron Station
Alexandria, VA 22314

1 Director
Defense Advanced Research
   Projects Agency
ATTN: LTC C. Fuck
1400 Wilson Boulevard
Arlington, VA 22209

2 Director
Inst for Defense Analysis
ATTN: H. Wolfhard
       R.T. Oliver
1801 Beauregard St.
Alexandria, VA 22311

1 Commander
US Army Materiel Development
   and Readiness Command
ATTN: DRCDMD-ST
5001 Eisenhower Avenue
Alexandria, VA 22333

2 Commander
US Army Armament Research
   and Development Command
ATTN: DRDAR-TSS
Dover, NJ 07801

4 Commander
US Army Armament Research
   and Development Command
ATTN: DRDAR-LCA, D. Downs
       DRDAR-LC, L. Harris
       DRDAR-SCA. L. Stiefel
       DRDAR-LCF, R.F. Walker
Dover, NJ 07801

1 Commander
US Army Armament Materiel
   Readiness Command
ATTN: DRSAR-LEP-L, Tech Lib
Rock Island, IL 61299

1 Director
US Army ARRADCOM
Benet Weapons Lab
ATTN: DRDAR-LCB-TL
Watervliet, NY 12189

1 Commander
US Army Waterviet Arsenal
ATTN: Code SARWV-RD,
           R. Thierry
Watervliet, NY 12189

1 Commander
US Army Aviation Research
   and Development Command
ATTN: **DRDAV-E**
4300 Goodfellow Blvd.
St. Louis, MO 63120

1 Director
US Army Air Mobility Research
   and Development Laboratory
Ames Research Center
Moffett Field, CA 94035

1 Commander
US Army Communications Rsch
   and Development Command
ATTN: DRDCO-PPA-SA
Fort Monmouth, NJ 07703

1 Commander
US Army Electronics Research
   and Development Command
Technical Support Activity
ATTN: DELSD-L
Fort Monmouth, NJ 07703

1 Commander
US Army Missile Command
ATTN: DRSMI-R
Redstone Arsenal, AL **35898**

1 Commander
US Army Missile Command
ATTN: DRSMI-YDL
Redstone Arsenal, AL **35898**

DISTRIBUTION LIST

No. of Copies	Organization	No. of Copies	Organization
1	Commander US Army Natick Research and Development Command ATTN: DRXRE, D. Sieling Natick, MA 01762	1	Commander Naval Sea Systems Command ATTN: J.W. Murrin, SEA-62R2 National Center Bldg. 2, Room 6E08 Washington, DC 20362
1	Commander US Army Tank Automotive Research & Development Cmd ATTN: DRDTA-UL Warren, MI 48090	1	Commander Naval Surface Weapons Center ATTN: Library Br., DX-21 Dahlgren, VA 22448
1	Commander US Army White Sands Missile Range ATTN: STEWS-VT White Sands, NM 88002	2	Commander Naval Surface Weapons Center ATTN: S.J. Jacobs/Code 240 Code 730 Silver Spring, MD 20910
1	Commander US Army Materials and Mechanics Research Center ATTN: DRXMR-ATL Watertown, MA 02172	1	Commander Naval Underwater Systems Cmd. Energy Conversion Department ATTN: R.S. Lazar/Code 5B331 Newport, RI 02840
5	Commander US Army Research Office ATTN: Tech Lib D. Squire F. Schmiedeshaff R. Ghirardelli M. Ciftan P. O. Box 12211 Research Triangle Park NC 27709	2	Commander Naval Weapons Center ATTN: R. Derr C. Thelen China Lake, CA 93555
1	Director US Army TRADOC Systems Analysis Activity ATTN: ATAA-SL, Tech Lib White Sands Missile Range NM 88002	1	Commander Naval Research Laboratory ATTN: Code 6180 Washington, DC 20375
1	Commander US Army Armament Research and Development Command ATTN: DRDAR-TDC Dover, NJ 07801	1	Commander Naval Research Laboratory Chem. Div. ATTN: J. McDonald Washington, DC 20375
		2	Office of Naval Research ATTN: Code 473 C. Neece 800 N. Quincy Street Arlington, VA 22217

DISTRIBUTION LIST

No. of Copies	Organization
3	Superintendent Naval Postgraduate School ATTN: Tech Lib D. Netzer A. Fuhs Monterey, CA 93940
2	Commander Naval Ordnance Station ATTN: Dr. Charles Dale Tech Lib Indian Head, MD 20640
2	AFOSR ATTN: D. Fall L. Caveny Bolling AFB, DC 20332
2	AFRPL (DYSC) ATTN: D. George J.N. Levine Edwards AFB, CA 93523
5	National Bureau of Standards ATTN: J. Hastie T. Kashiwagi H. Senerjian M. Jacox J. Stevenson Washington, DC 20234
1	General Motors Rsch Labs Physics Department ATTN: J.H. Bechtel Warren, Michigan 48090
1	Lockheed Missiles & Space Co. ATTN: Tech Info Ctr 3251 Hanover Street Palo Alto, CA 94304
1	System Research Labs ATTN: L. Goss 2600 Indian Ripple Rd Dayton, Ohio 45440

No. of Copies	Organization
1	Aerojet Solid Propulsion Co. ATTN: P. Micheli Sacramento, CA 95813
1	ARO Incorporated Arnold AFB, TN 37389
1	Atlantic Research Corporation ATTN: M.K. King 5390 Cherokee Avenue Alexandria, VA 22314
1	AVCO Everett Research Lab ATTN: D. Stickler 2385 Revere Beach Parkway Everett, MA 02149
2	Calspan Corporation ATTN: E.E. Fisher A.P. Trippe P.O. Box 400 Buffalo, NY 14225
2	Exxon Research & Engineering ATTN: A. Dean M. Chou P.O. Box 45 Linden, NJ 07036
1	Foster Miller Associates, Inc ATTN: A.J. Erickson 135 Second Avenue Waltham, MA 02154
1	General Electric Company Armament Department ATTN: M.J. Bulman Lakeside Avenue Burlington, VT 05402
1	General Electric Company Flight Propulsion Division ATTN: Tech Lib Cincinnati, OH 45215
1	Sandia National Laboratories ATTN: D. Stephenson Div. 8351 Livermore, CA 94550

DISTRIBUTION LIST

No. of Copies	Organization	No. of Copies	Organization
1	General Electric Corp. R&D ATTN: N. Drake P.O. Box8, Bldg, K1, Rm. 51326 Schenectady, N.Y. 12301	1	Pulsepower Systems, Inc. ATTN: L.C. Elmore 815 American Street San Carlos, CA 94070
2	Hercules Incorporated **Allegheny** Ballistic Lab ATTN: R. Miller Tech Lib Cumberland, MD **21501**	3	Rockwell International Corp. Rocketdyne Division ATTN: C. Obert J.E. Flanagan A. Axeworthy 6633 Canoga Avenue Canoga Park, CA 91304
1	Hercules Incorporated Bacchus Works ATTN: B. Isom Magna, UT 84044	2	Hercules, Inc. **Industrial Systems Dept.** ATTN: Tech Lib P. O. Box 548 **McGregor, TX 76657**
1	IBM Corp ATTN: A.C. Tam Research Div. 5600 Cottle Rd San Jose, CA 95193	1	Science Applications, Inc ATTN: R.B. Edelman Combustion Dynamics & Propulsion Division 23146 Cumorah Crest Woodland Hills, CA 91364
1	IITRI ATTN: M.J. Klein 10 West 35th Street Chicago, IL **60616**	1	Shock Hydrodynamics, Inc ATTN: W.H. Anderson 4710-16 Vineland Avenue N. Hollywood, CA 91602
1	Olin Corporation Badger Army Ammunition Plant ATTN: J. Ramnarace Baraboo, WI 53913	1	Thiokol Corporation Elkton Division ATTN: E. Sutton Elkton, MD 21921
1	Olin Corporation New Haven Plant 275 Winchester Ave. New Haven, CT 06504	3	Thiokol Corporation Huntsville Division ATTN: D. Flanigan R. Glick Tech Lib Huntsville, AL 35807
1	Paul Gough Associates, Inc ATTN: P.S. Gough P.O. Box 1614 Portsmouth, NH 03801	2	Thiokol Corporation Wasatch Division ATTN: J. Peterson Tech Lib P.O. Box 524 Brigham City, UT 84302
1	Physics International Co 2700 Merced Street Leandro, CA 94577		

DISTRIBUTION LIST

No. of Copies	Organization	No. of Copies	Organization
1	TRW Systems Group ATTN: H. Korman One Space Park Redondo Beach, CA 90278	1	Institute of Gas Technology ATTN: D. Gidaspow 3424 S. State Street Chicago, IL 60616
2	United Technologies Chemical Systems Division ATTN: R. Brown Tech Lib P.O. Box 358 Sunnyvale, CA 94086	1	Johns Hopkins University/APL Chemical Propulsion Info Ap ATTN: T. Christian Johns Hopkins Road Laurel, MD 20810
3	Battelle Memorial Institute ATTN: Tech Lib 505 King Avenue Columbus, OH 43201	1	Massachusetts Inst. of Tech Dept of Mech Engineering ATTN: T. Toong Cambridge, MA 02139
2	Brigham Young University Dept of Chemical Engineering ATTN: M.W. Beckstead Provo, UT 84601	2	Pennsylvania State University Dept of Mechanical Eng ATTN: K. Kuo G. Faeth University Park, PA 16802
1	California Institute of Tech 204 Karmar Lab Mail Stop 301-46 ATTN: F.E.C. Culick 1201 E. California Street Pasadena, CA 91125	1	Pennsylvania State University Dept of Material Sciences ATTN: H. Palmer University Park, PA 16802
1	Case Western Reserve Univ Aerospace Sciences ATTN: J. Tien Cleveland, OH 44135	1	Polytechnic Institute of NY ATTN: S. Lederman Route 110 Farmingdale, NY 11735
1	Cornell University Department of Chemistry ATTN: L. Grant Baker Laboratory Ithaca, N.Y. 14850	1	Princeton Combustion Research Labortories ATTN: M. Summerfield 1041 U.S. Highway One North Princeton, NJ 08540
3	Georgia Institute of Tech School of Aerospace Eng. ATTN: B.T. Zinn F. Price W.C. Strahle Atlanta, GA 30332	3	Princeton University Forrestal Campus ATTN: I. Glassman K. Brezinsky Tech Lib P.O. Box 710 Princeton, NJ 08540

DISTRIBUTION LIST

No. of Copies	Organization	No. of Copies	Organization
4	Purdue University School of Mechanical Eng. ATTN: J. Osborn S.N.P. Murphy N.M. Laurendeau D. Sweeney TSPC Chaffee Hall W. Lafayette, IN 47906	1	University of California Dept. of Mechanical Eng. ATTN: J.W. Daily Berkeley, California 94720
1	Rensselaer Polytecnic Inst. Dept. of Chem. Engineering ATTN: A. Fonijn Troy, NY 12181	1	Univ. of Dayton Rsch Inst ATTN: D. Campbell AFRPL/PAP Stop 24 Edwards Air Force Base, CA 93523
1	Rutgers State University Dept of Mechanical and Aerospace Engineering ATTN: S. Temkin University Heights Campus New Brunswick, NJ 08903	1	University of Florida Dept. of Chemistry ATTN: J. Winefordner Gainesville, Florida 32601
1	Sandia Laboratories Combustion Sciences Dept. ATTN: R. Cattolica Livermore, CA 94550	1	University of Illinois Dept of Mechanical Eng. . ATTN: H. Krier 144 MEB, 1206 W Green St. Urbana, IL 61801
4	SRI International ATTN: Tech Lib D. Crosley J. Barker D. Golden 333 Ravenswood Avenue Menlo Park, CA 94025	1	University of Minnesota Dept of Mechanical Eng. ATTN: E. Fletcher Minneapolis, MN 55455
1	Stevens Institute of Tech Davidson Library ATTN: R. McAlevy, III Hoboken NJ 07030	1	University of Southern California Department of Chemistry ATTN: S. Benson Los Angeles, CA 90007
1	University of California, San Diego Ames Department ATTN: F. Williams P.O. Box 109 La Jolla, CA 92037	2	University of Texas Department of Chemistry ATTN: W. Gardiner H. Schaefer Austin, TX 78712
		2	University of Utah Dept. of Chemical Engineering ATTN: A. Baer G. Flandro Salt Lake City, UT 84112
		1	United Technologies ATTN: A. C. Eckbreth East Hartford, CT 06108

DISTRIBUTION LIST

No. of
Copies   Organization

Aberdeen Proving Ground

Dir, USAMSAA
  ATTN: DRXSY-D
        DRXSY-MP, H. Cohen
Cdr, USATECOM
  ATTN: DRSTE-TO-F
Dir, USACSL, Bldg E3516
  ATTN; DRDAR-CLB-PA

USER EVALUATION OF REPORT

Please take a few minutes to answer the questions below; tear out
this sheet, fold as indicated, staple or tape closed, and place
in the mail. Your comments will provide us with information for
improving future reports.

1. BRL Report Number_____

2. Does this report satisfy a need? (Comment on purpose, related
project, or other area of interest for which report will be used.)

_____

_____

_____

3. How, specifically, is the report being used? (Information
source, design data or procedure, management procedure, source of
ideas, etc.)_____

_____

_____

4. Has the information in this report led to any quantitative
savings as far as man-hours/contract dollars saved, operating costs
avoided, efficiencies achieved, etc.? If so, please elaborate.

_____

_____

5. General Comments (Indicate what you think should be changed to
make this report and future reports of this type more responsive
to your needs, more usable, improve readability, etc.)_____

_____

_____

_____

6. If you would like to be contacted by the personnel who prepared
this report to raise specific questions or discuss the topic,
please fill in the following information.

              Name:_____

    Telephone Number:_____

Organization Address:_____

                      _____

                      _____

DATE
FILMED

7-8